Using Singular Value Decomposition to Analyze Drug/beta-Cyclodextrin Mixtures: Insight from X-ray Powder Diffraction Patterns

Kanji Hasegawa; Satoru Goto*; Chihiro Tsunoda ; Chihiro Kuroda; Yuta Okumura; Ryosuke Hiroshige; Ayako Wada-Hirai; Shota Shimizu; Hideshi Yokoyama; and Tomohiro Tsuchida

Faculty of Pharmaceutical Sciences, Tokyo University of Science

Supplemental Materials
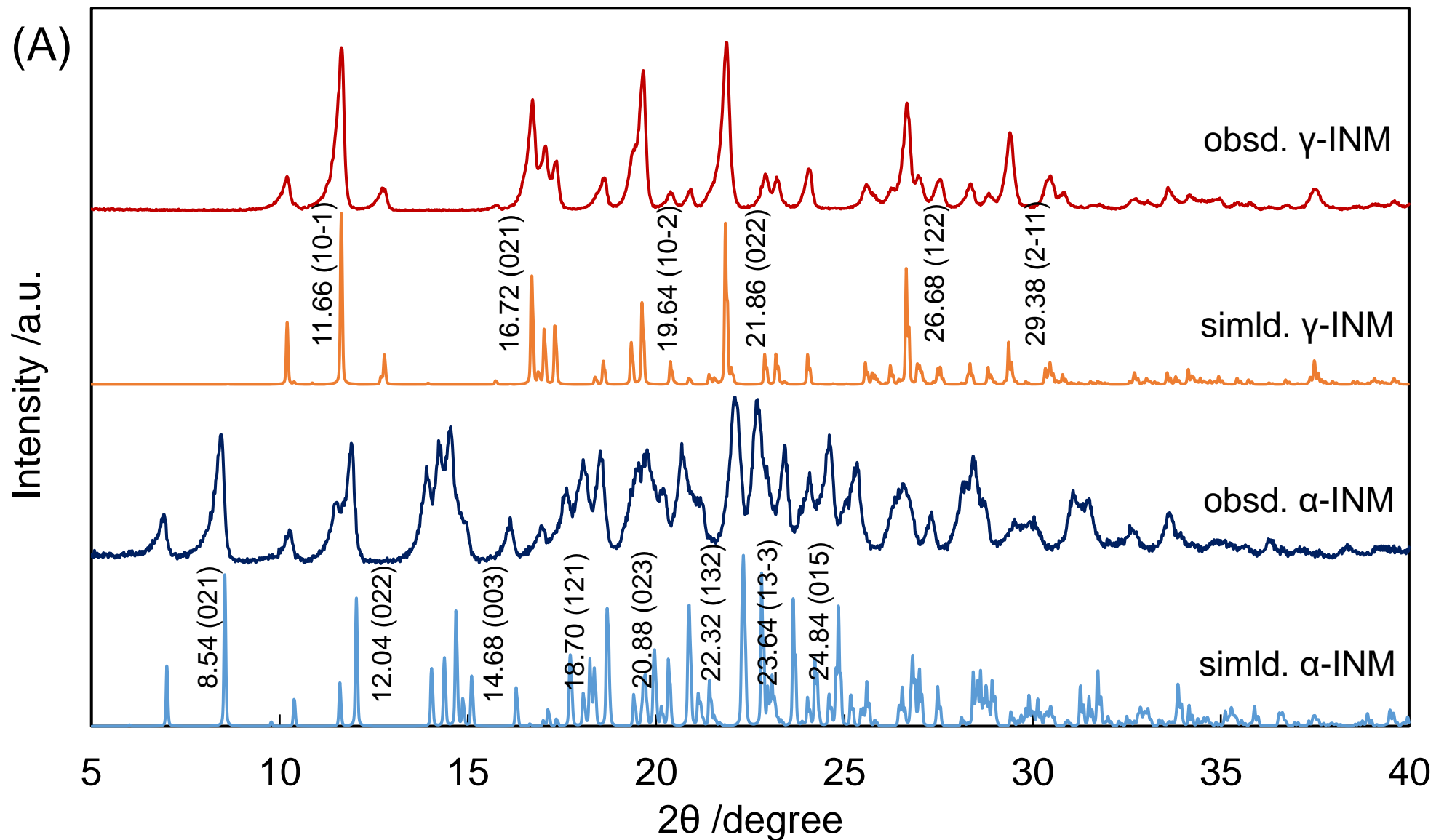
Figure S2(A) The simulated diffractograms of γ- (orange) and α-INM (blue). The corresponding CCDC entries are INDMET (T.J. Kistemmacher & R.E. Marsh, 1972) and INDMET04 (M. Arisawa, et al 2011). Numbers were presented 2θ angles and Miller indexes *h*, *k*, and *l* were in parenthesis.
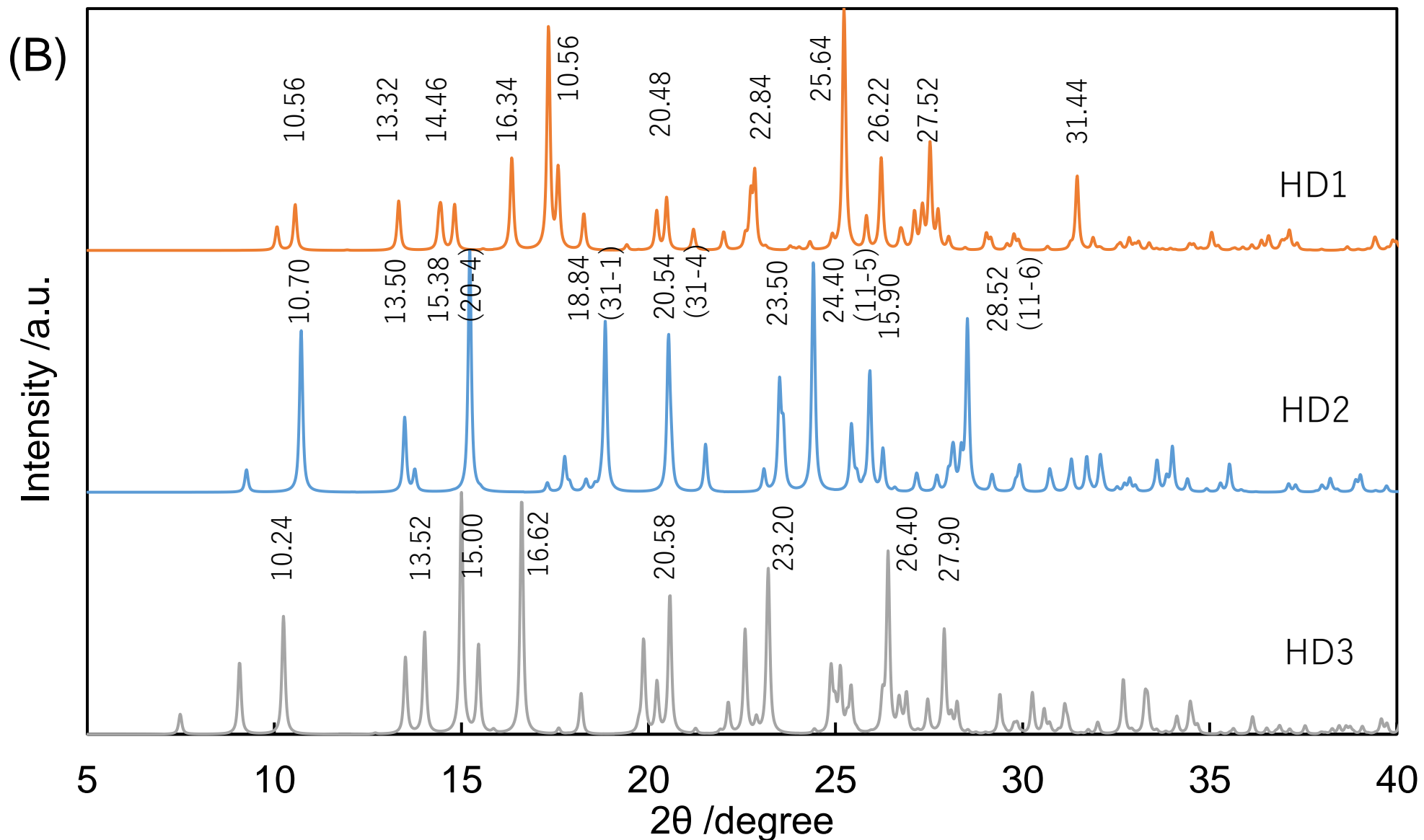
Figure S2(B) The simulated diffractograms of DCF. The corresponding CCDC entries are SIKLIH (P. Moster, et al. 1990) for HD1 crystal, SIKLIH02 (C. Castellari & A. Ottani, 1997) for HD1 , and SIKLIH04 (N. Jaiboon, et al. 2001) for HD3. Numbers were presented 2θ angles and Miller indexes *h*, *k*, and *l* were in parenthesis.

(C)

Intensity /a.u.

A-FAM

7.48 (100)
10.72 (002)
14.43 (110)
17.16 (11-2)
18.7 (112)
20.24 (013)
23.28 (30-2)

B-FAM

6.00 (100)
11.62 (002)
15.14 (30-2)
15.78 (102)
17.66 (11-1)
18.08 (300)
19.38 (11-2)
20.18 (21-2)
20.66 (210)
20.92 (202)
22.38 (21-3)
22.64 (31-2)
23.80 (31-3)
24.18 (400)
24.72 (310)
26.32 (41-2)
26.60 (41-3)
27.24 (104)
30.24 (20-6)
32.34 (402)

2θ /degree
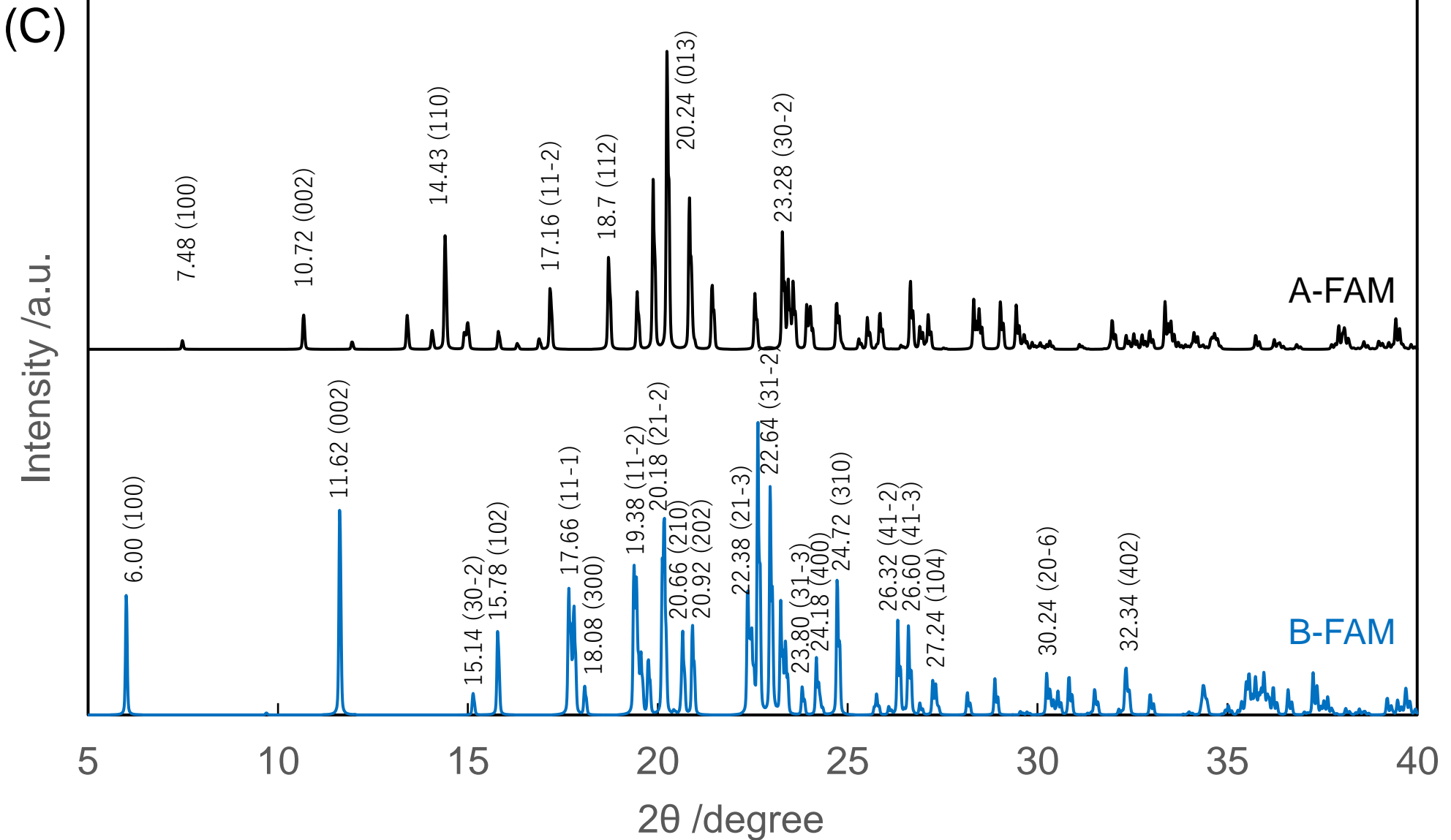
Figure S2(C) The simulated diffractograms of A- (black) and B-FAM (blue). The corresponding CCDC entries are FOGVIG01 (L. Golic, *et al.*, 1989) and FOGVIG02 (K. Shankland, *et al.* , 2002). Numbers were presented 2θ angles and Miller indexes *h*, *k*, and *l* were in parenthesis.
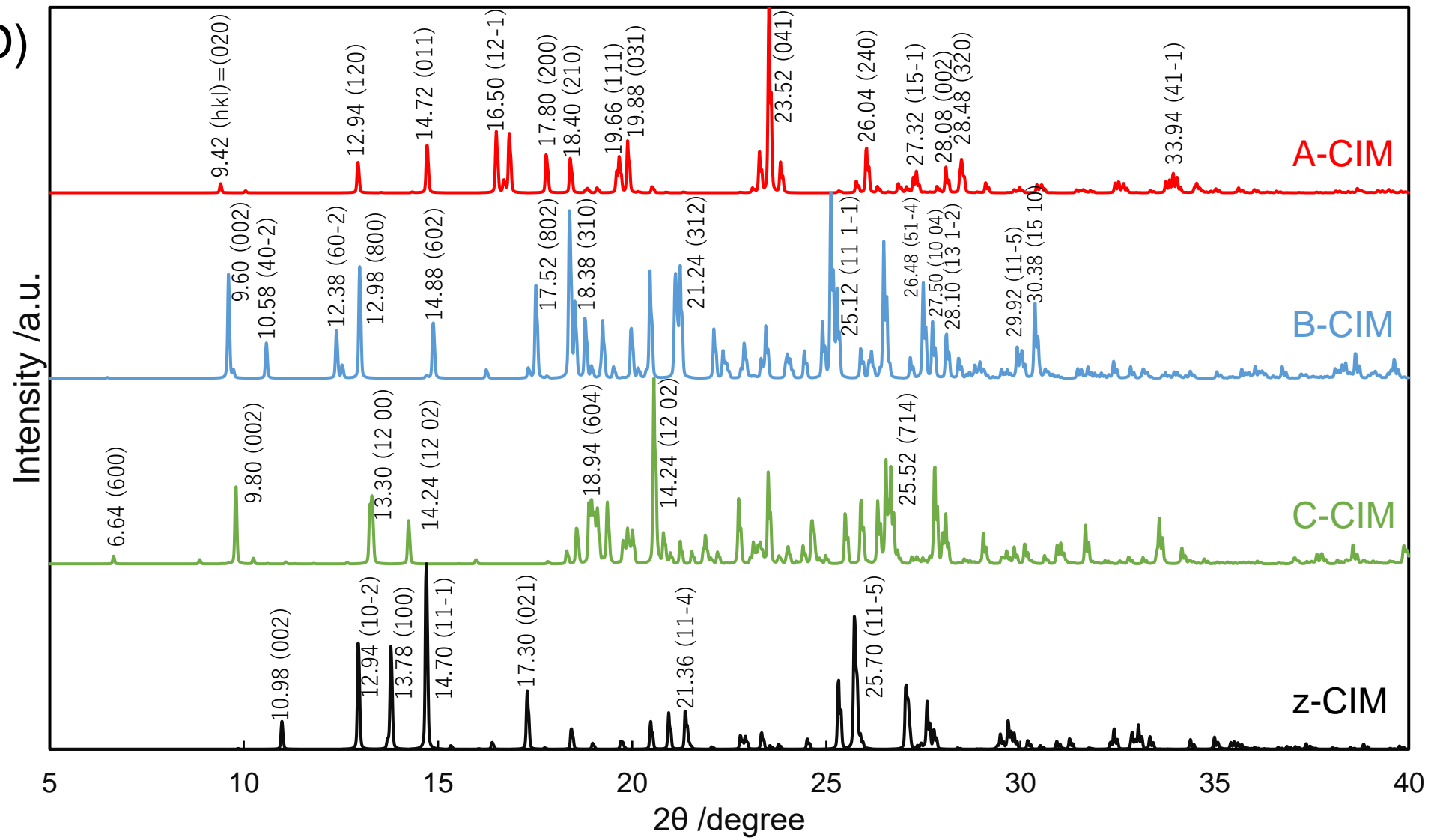
Figure S2(D) The simulated diffractograms of A- (red), B- (blue), C- (green) and z-CIM (black). The corresponding CCDC entries are CIMETD02 (S.R. Critchley, 1979), CIMETD06 (M.C.G. Afonso, *et al.*, 2019), CIMETD04 (A. Arakcheeva, *et al.*, 2013) and CIMETD01 (L.Parkanyi, *et al.*, 1984).
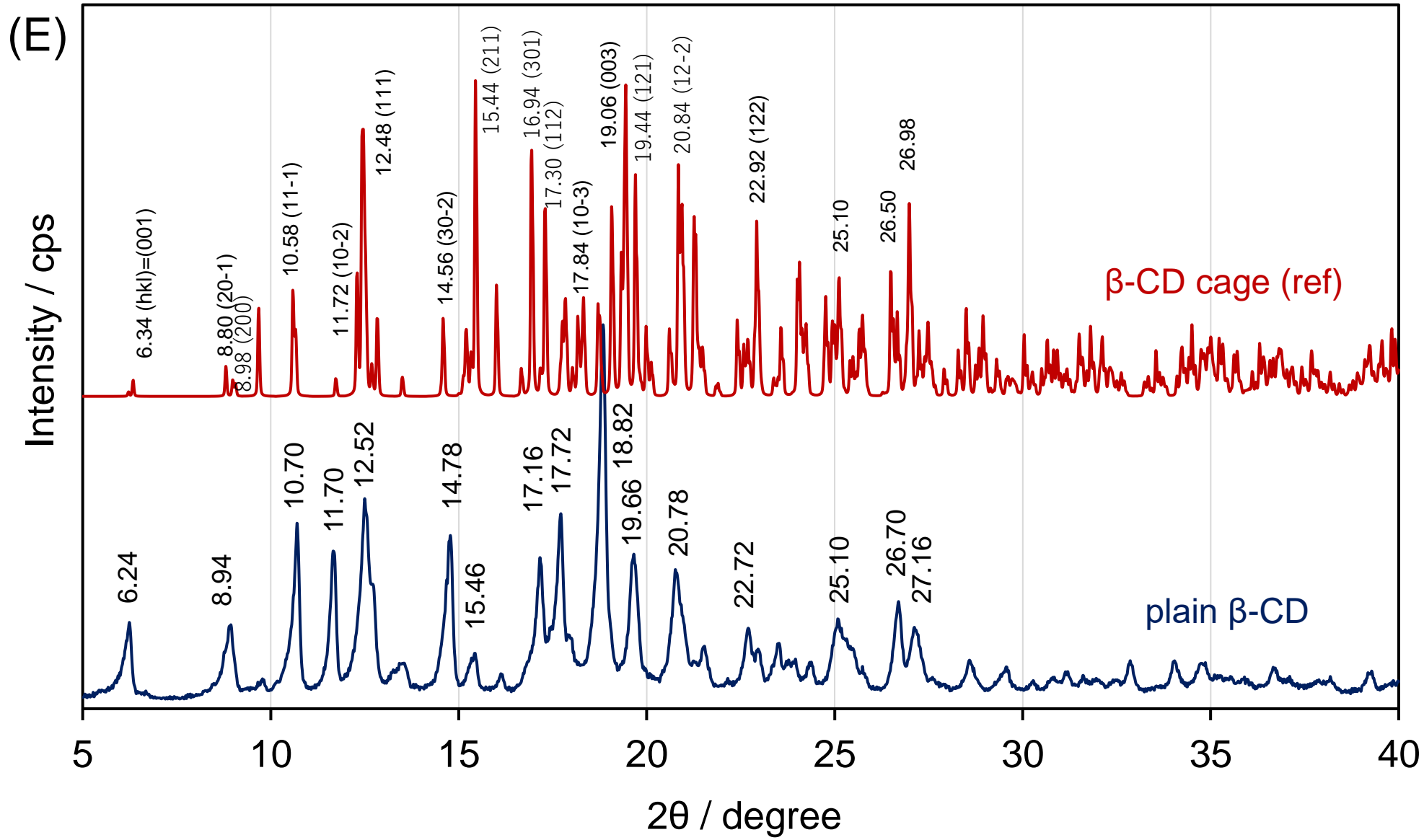
Figure S2(E) The simulated diffractograms of the β-CyD cage (burgundy), corresponding to the CCDC entry BCDEXD03 (T.Steiner *et al.*, 1994), and the observed pattern of the plain β-CD with a cage form.
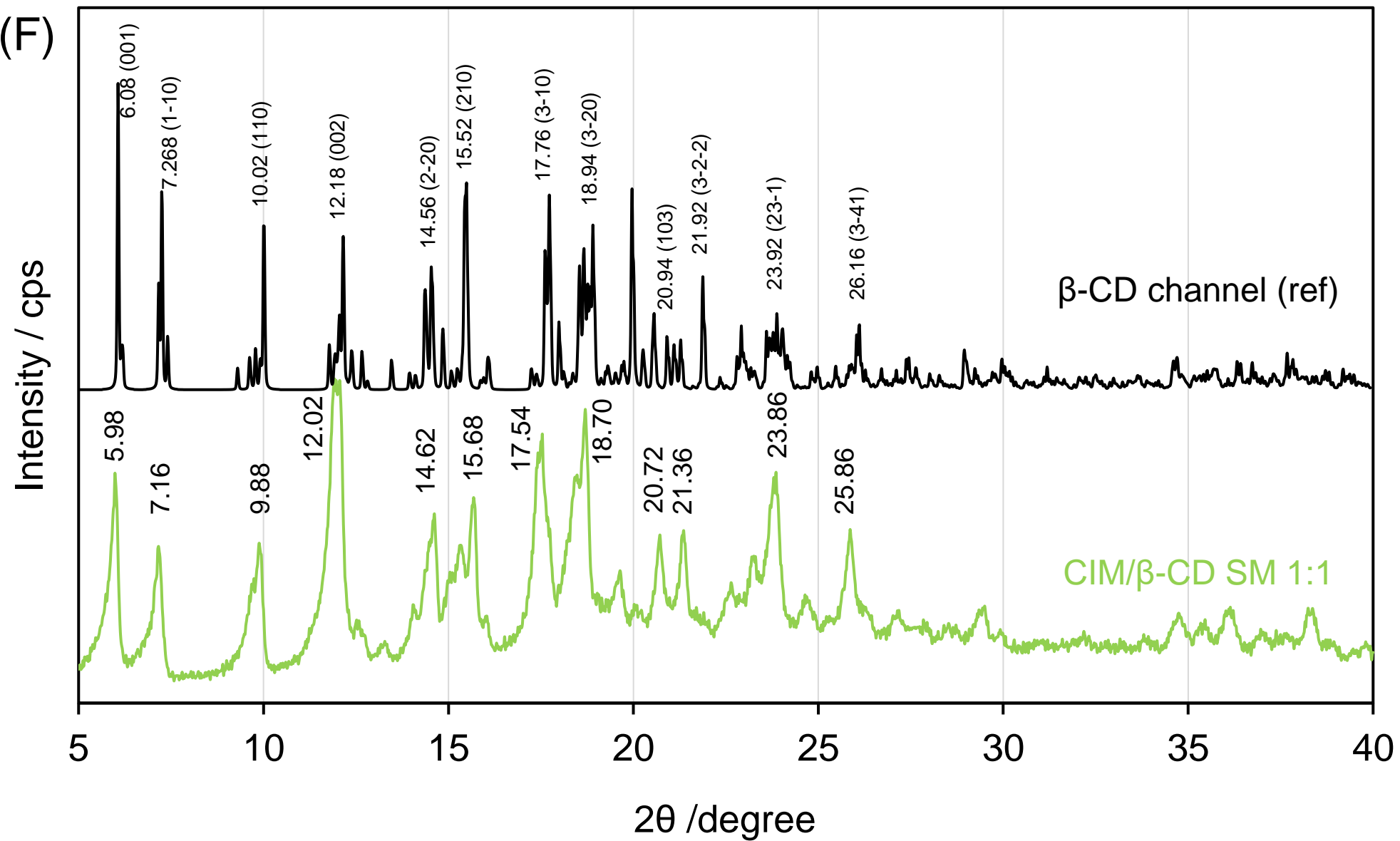
Figure S2(F) The simulated diffractograms of the β-CyD channel (black) corresponding to the CCDC entry OFAXID (E-J. Wang *et al.,*2007), and the observed pattern of CIM/β-CD with a channel form.

plain β-CD in DMSO-d_6

Hydroxyl-proton (OH2, OH3, and OH6) signals appeared in the aprotic solvent DMSO. So, signals of aliphatic protons involved the fine structures corresponding to these coupling with the OH-protons, providing complex signals.
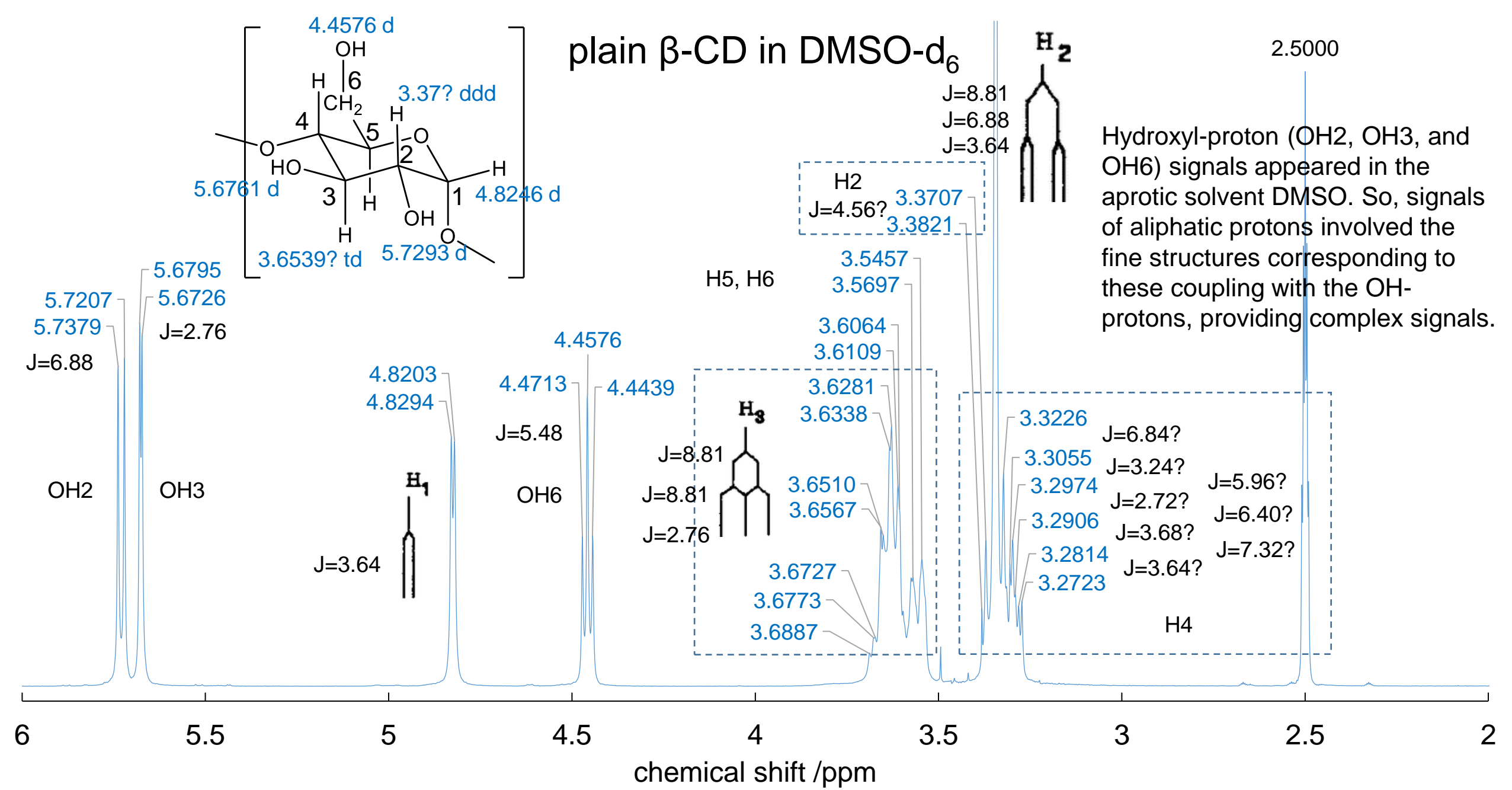
Figure S3(A) The 400 MHz ^{1}H-NMR spectrum of the plain β-CD in DMSO-d_6
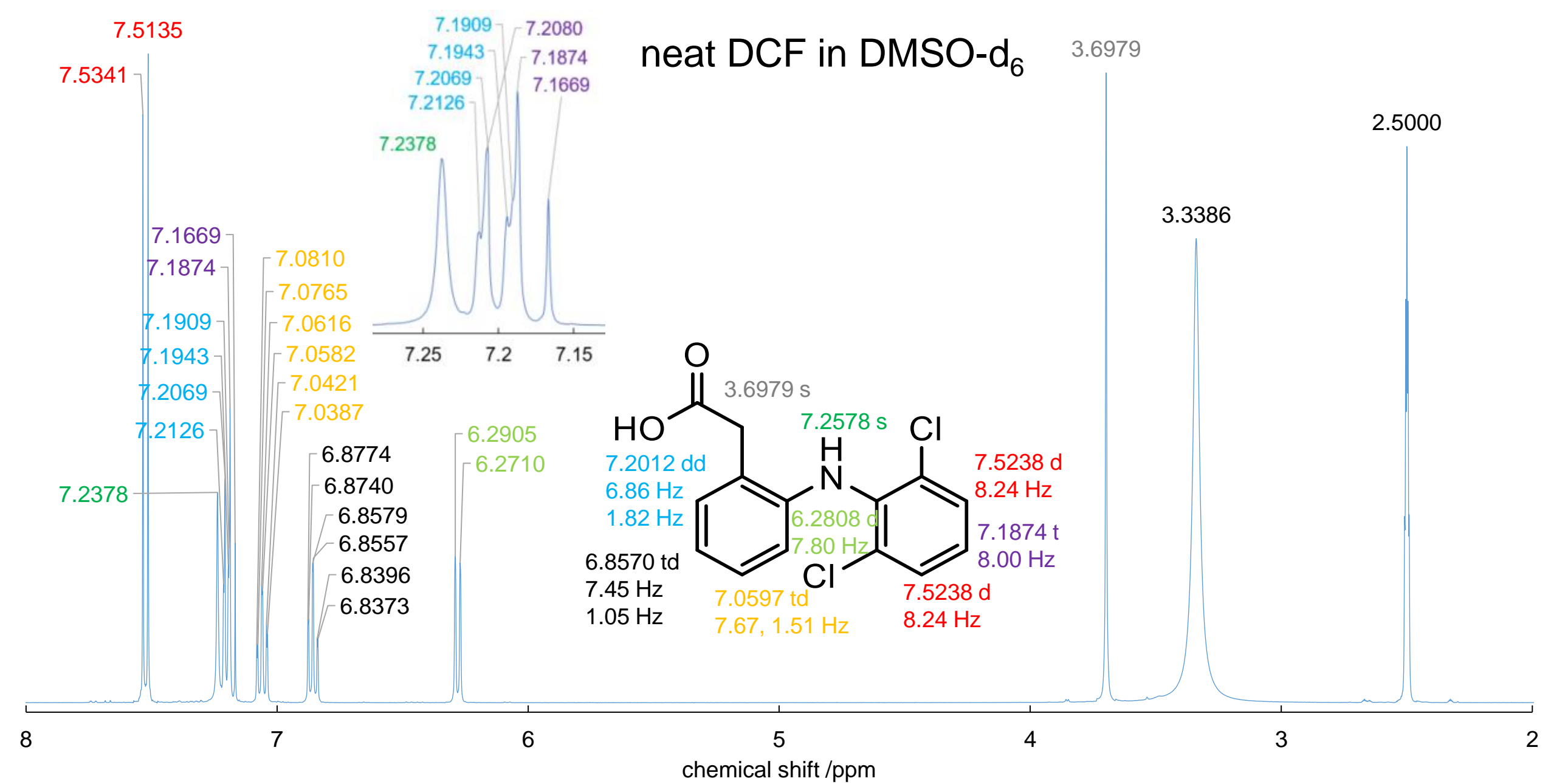
Figure S3(B) The 400 MHz ^{1}H-NMR spectrum of the neat DCF in DMSO-d$_6$
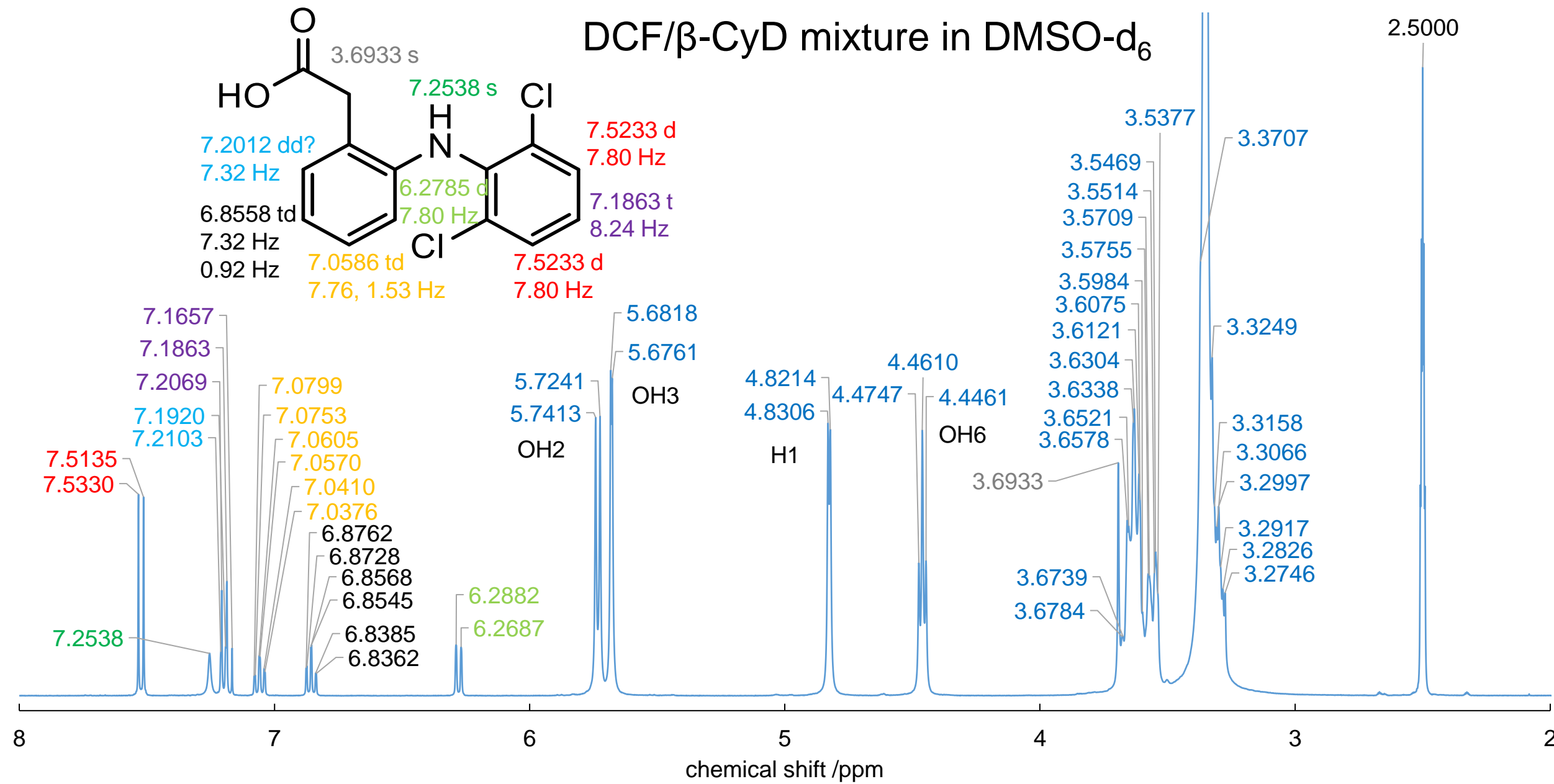
Figure S3(C) The 400 MHz ^{1}H-NMR spectrum of the DCF/β-CD mixture in DMSO-d$_6$

neat FAM in DMSO-d$_6$
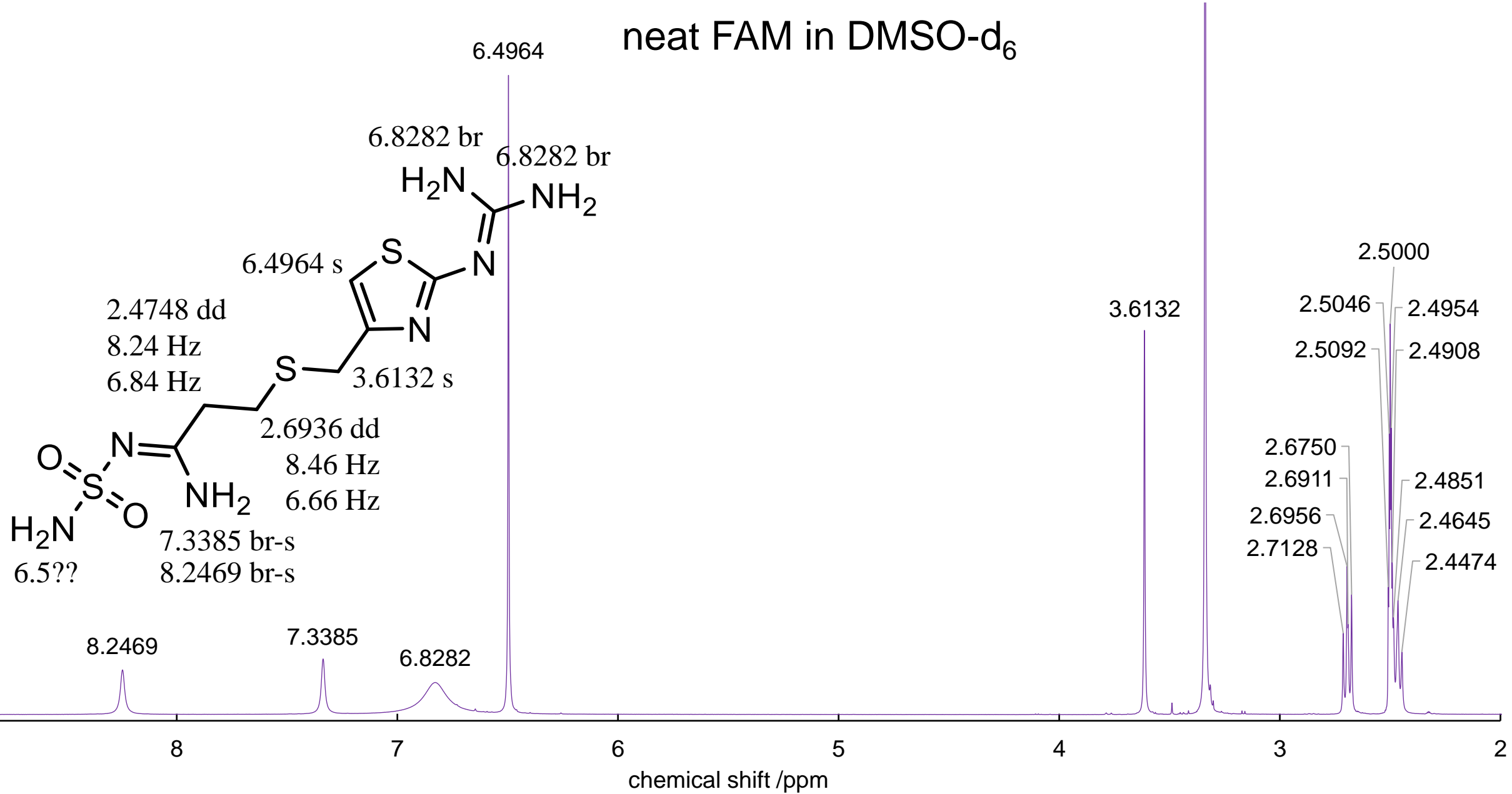
Figure S3(D) The 400 MHz ^{1}H-NMR spectrum of the neat FAM in DMSO-d$_6$
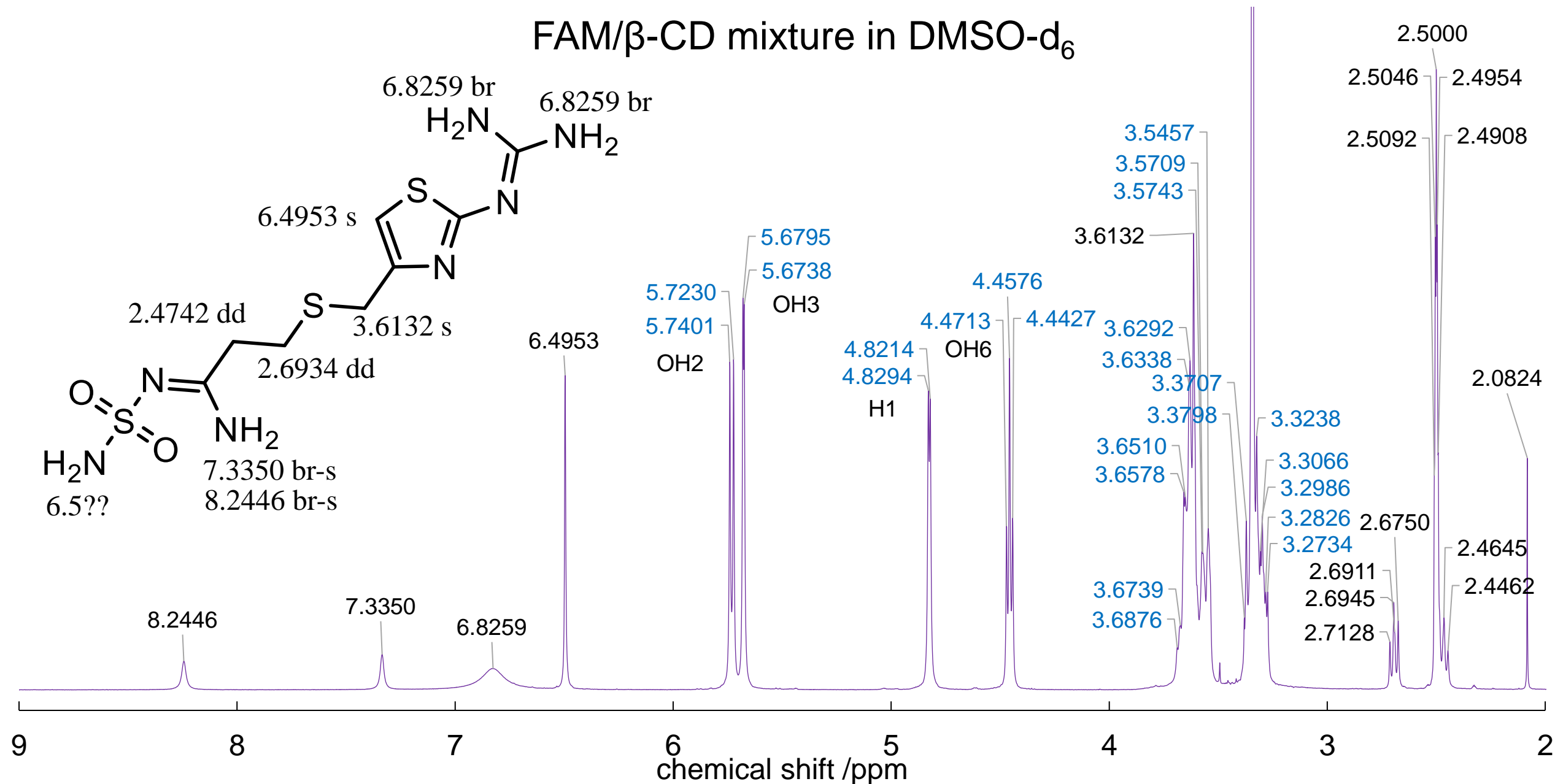
Figure S3(E) The 400 MHz ^{1}H-NMR spectrum of the FAM/β-CD mixture in DMSO-d$_6$
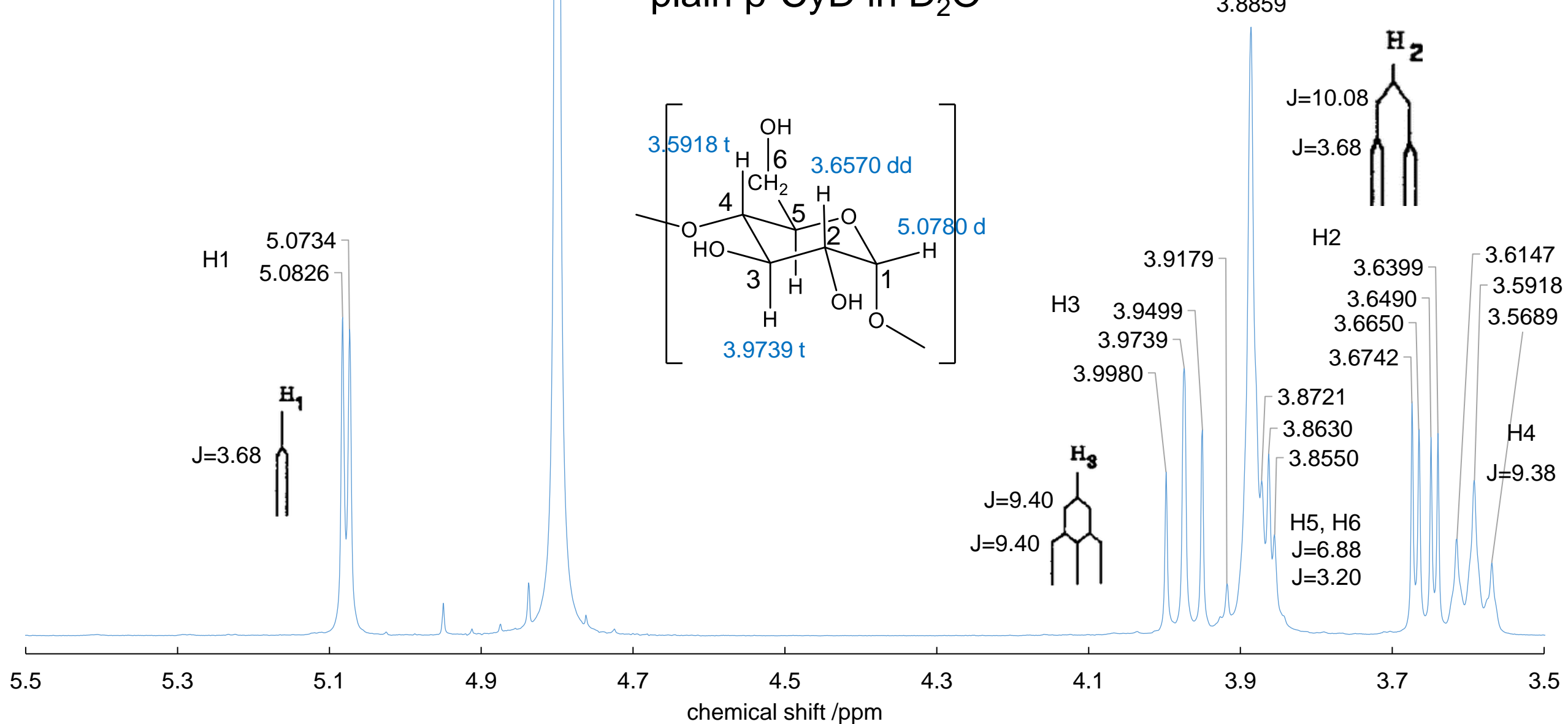
Figure S4(A) The 400 MHz ^{1}H-NMR spectrum of the plain β-CD in D_2O (at 4.8000 ppm)

plain β-CyD in D_2O

13
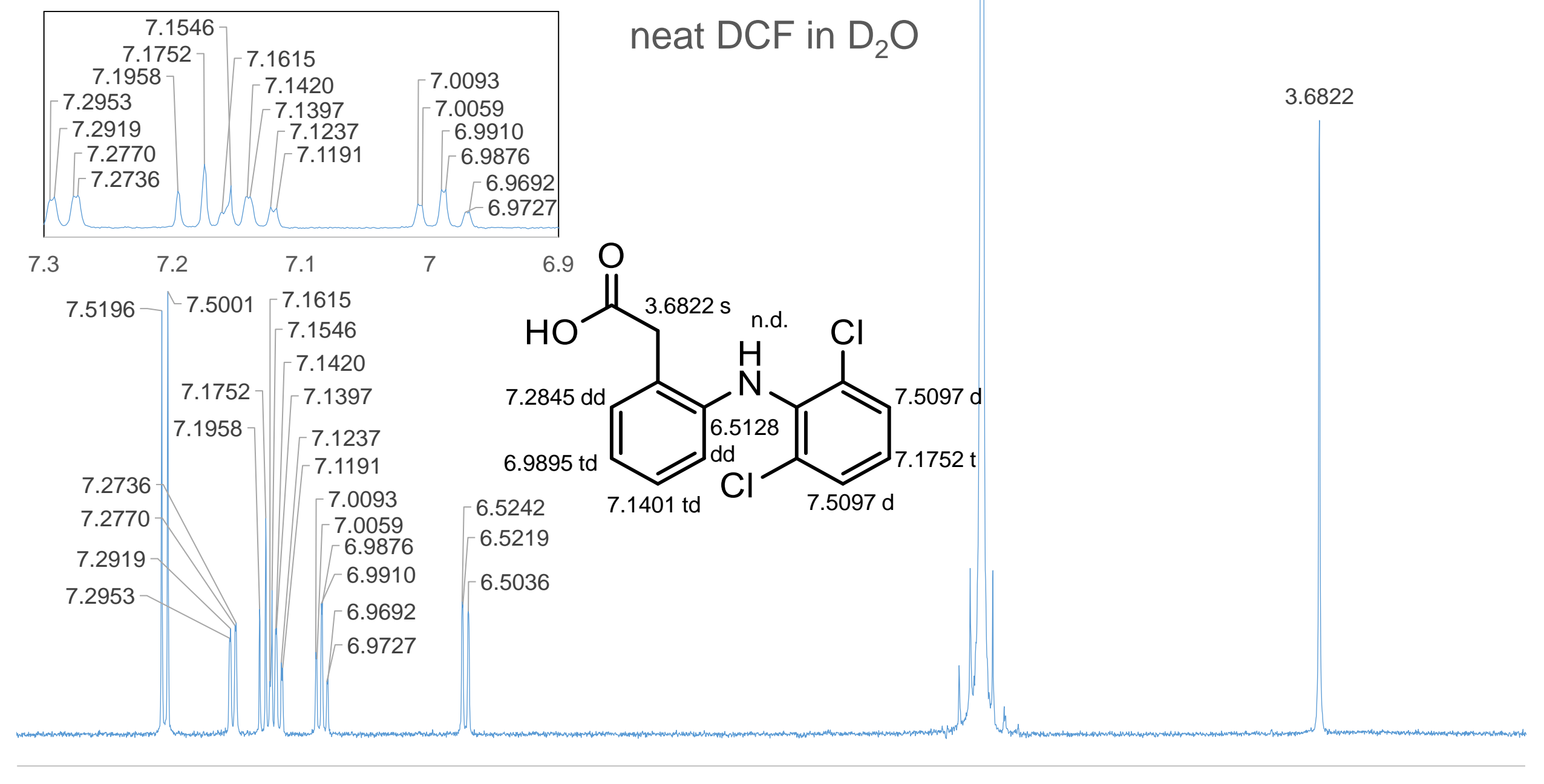
Figure S4(B) The 400 MHz ^{1}H-NMR spectrum of the neat DCF in D_2O (at 4.8000 ppm)

14
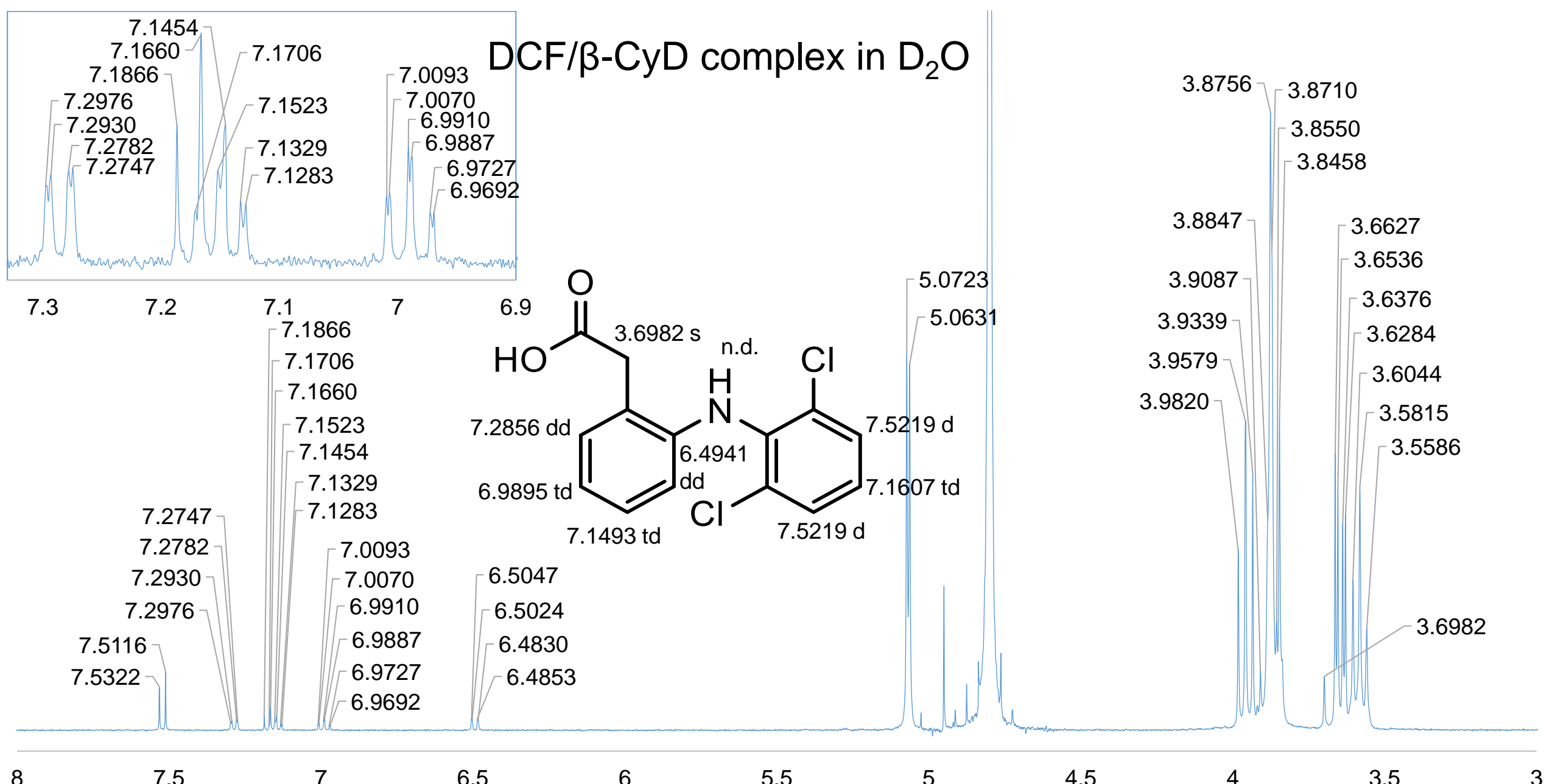
Figure S4(C) The 400 MHz ¹H-NMR spectrum of the DCF/β-CD complex in D_2O (at 4.8000 ppm)[15]
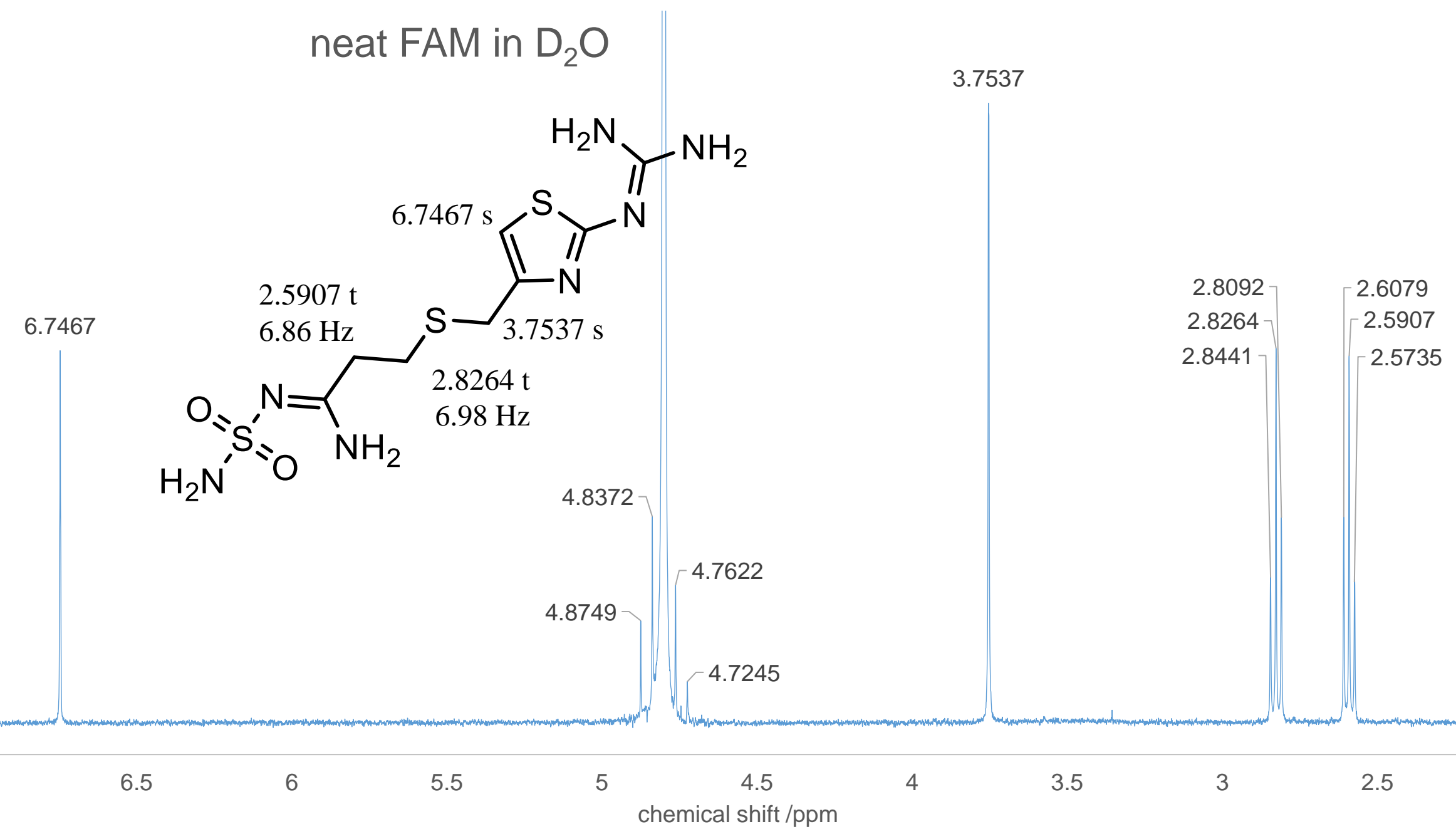
Figure S4(D) The 400 MHz ^{1}H-NMR spectrum of the neat FAM in D_2O (at 4.8000 ppm)
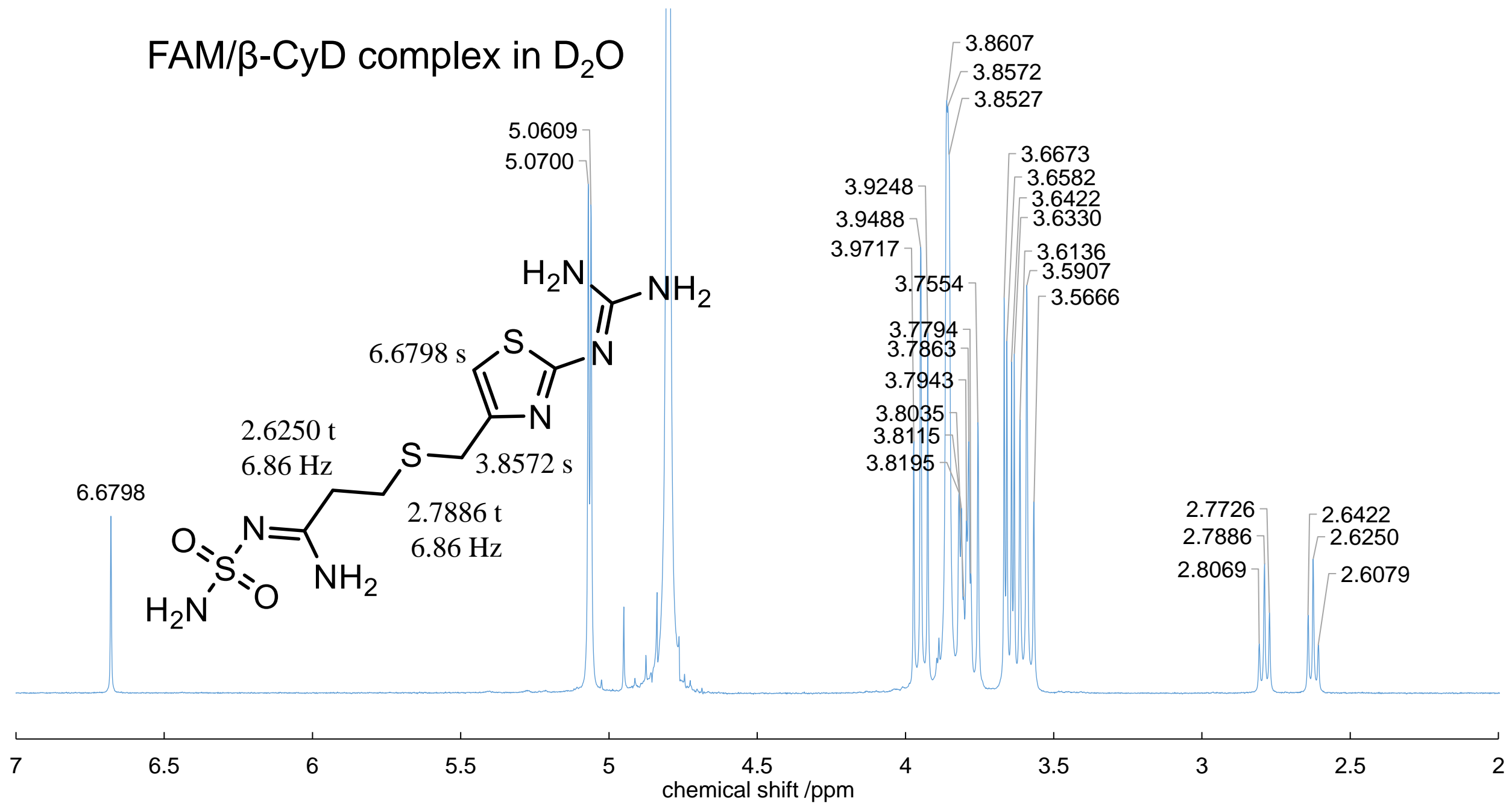
Figure S4(E) The 400 MHz ^{1}H-NMR spectrum of the FAM/β-CD complex in D$_2$O (at 4.8000 ppm)[17]
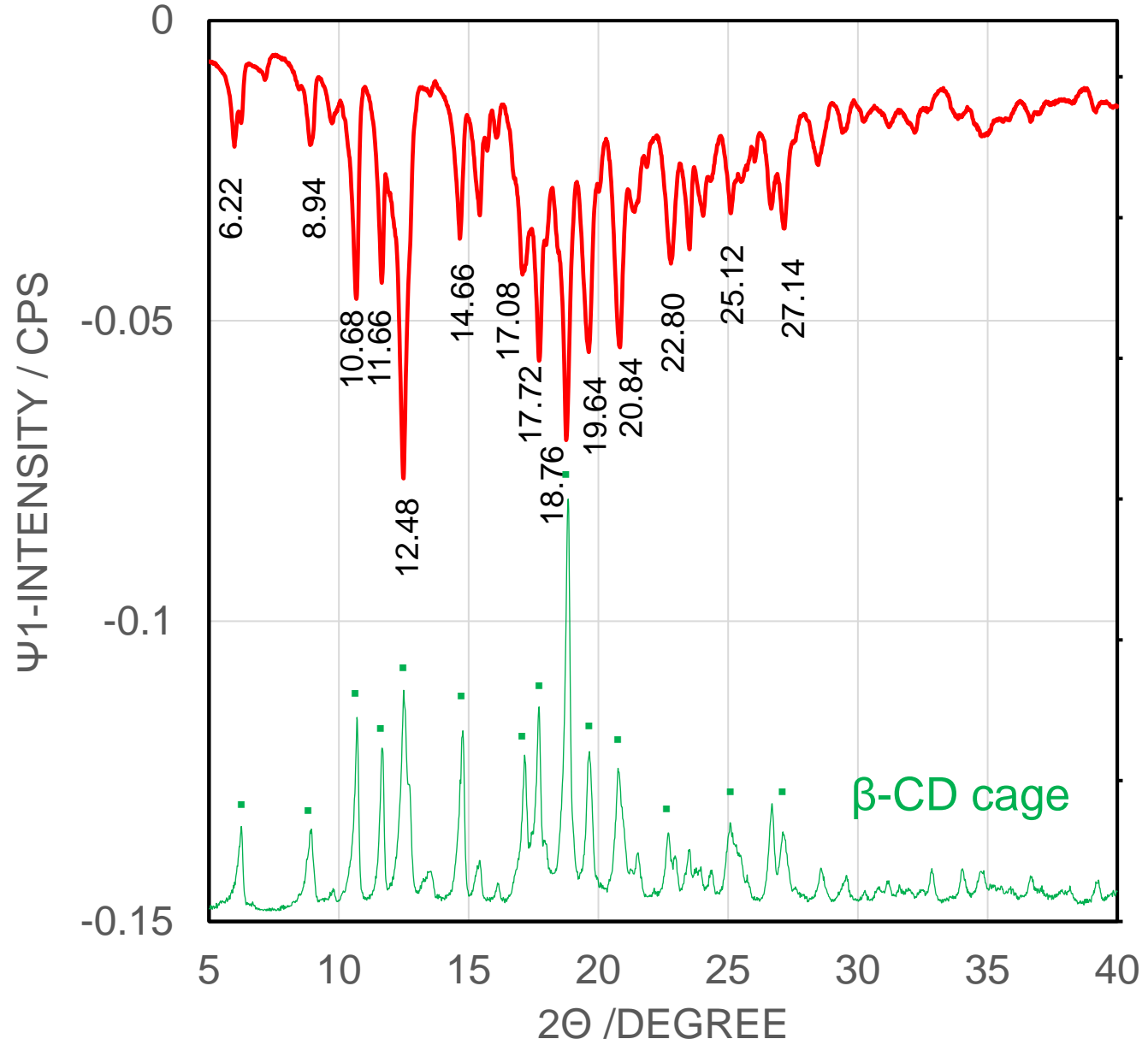
Figure S5(A) The 1-st singular vector (red) in the SVD for the diffractograms of API/β-CD mixtures, compared with the diffractogram of β-CD cage form (green)
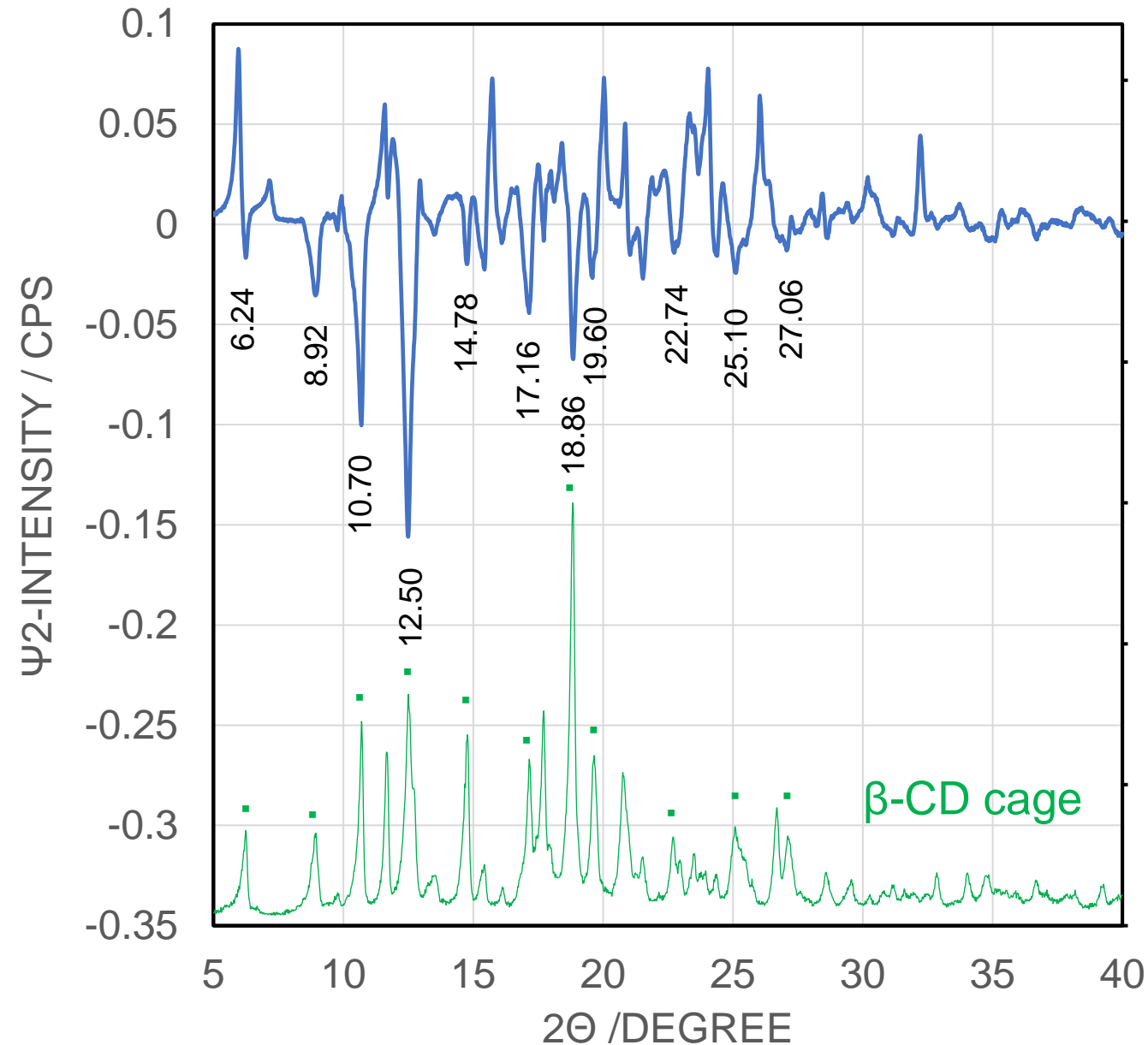
Figure S5(B) The 2-nd singular vector (blue) compared with the diffractogram of β-CD cage form (green)
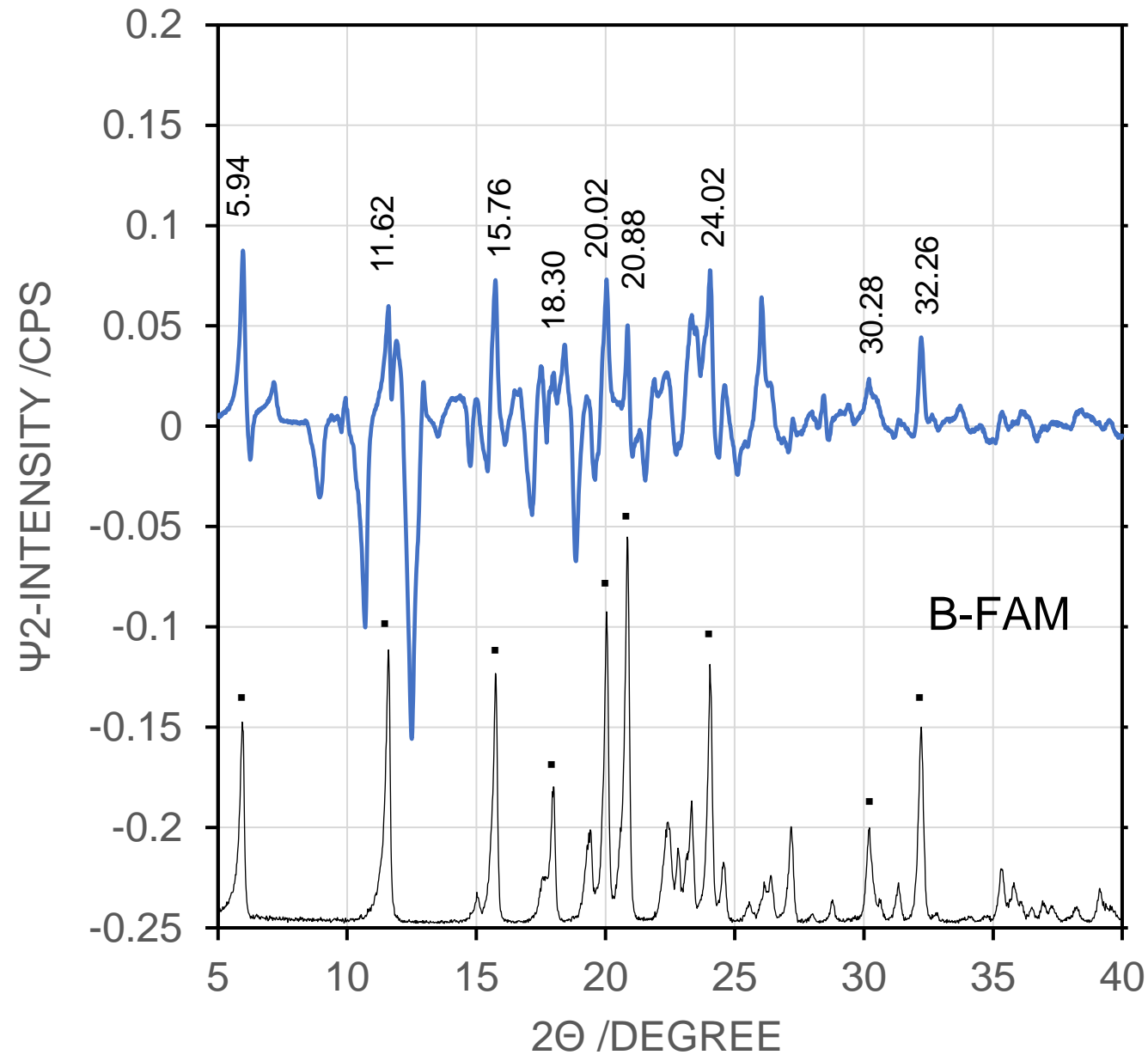
Figure S5(C) The 2-nd singular vector (blue) compared with the diffractogram of FAM B-form (black)   20
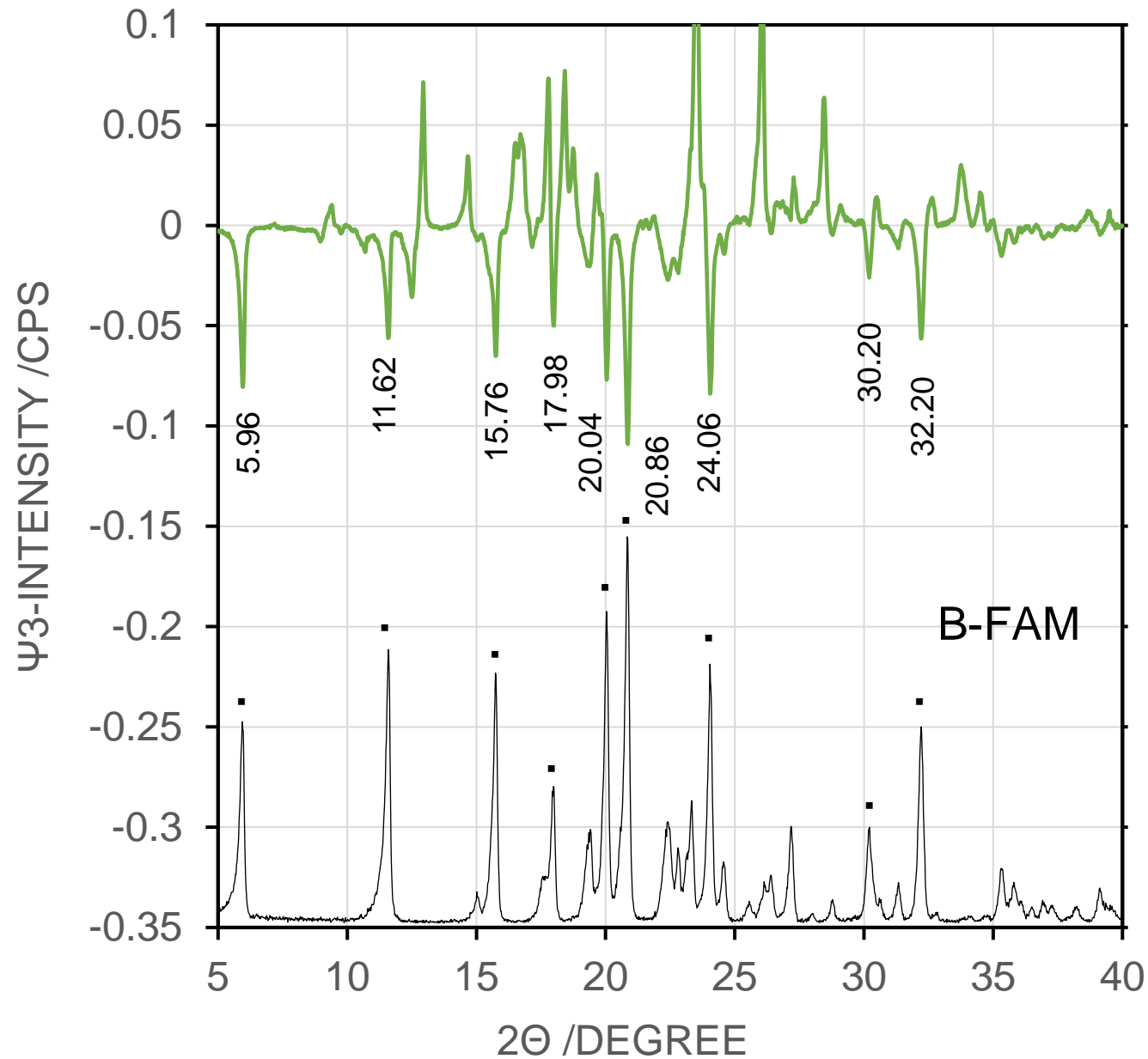
Figure S5(D) The 3-rd singular vector (green) compared with the diffractogram of FAM B-form (black) 21
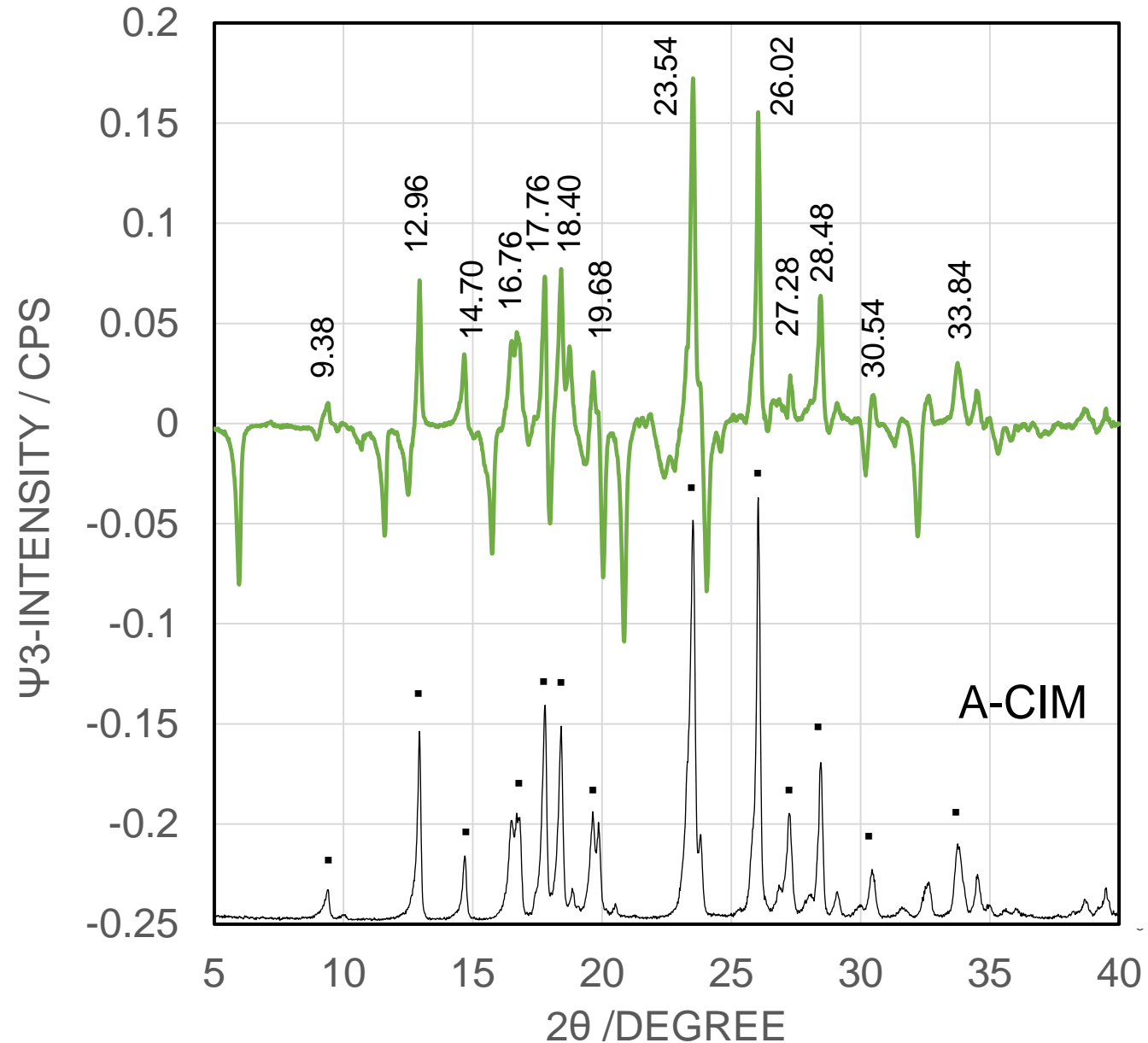
Figure S5(E) The 3-rd singular vector (green) compared with the diffractogram of CIM A-form (black)   22
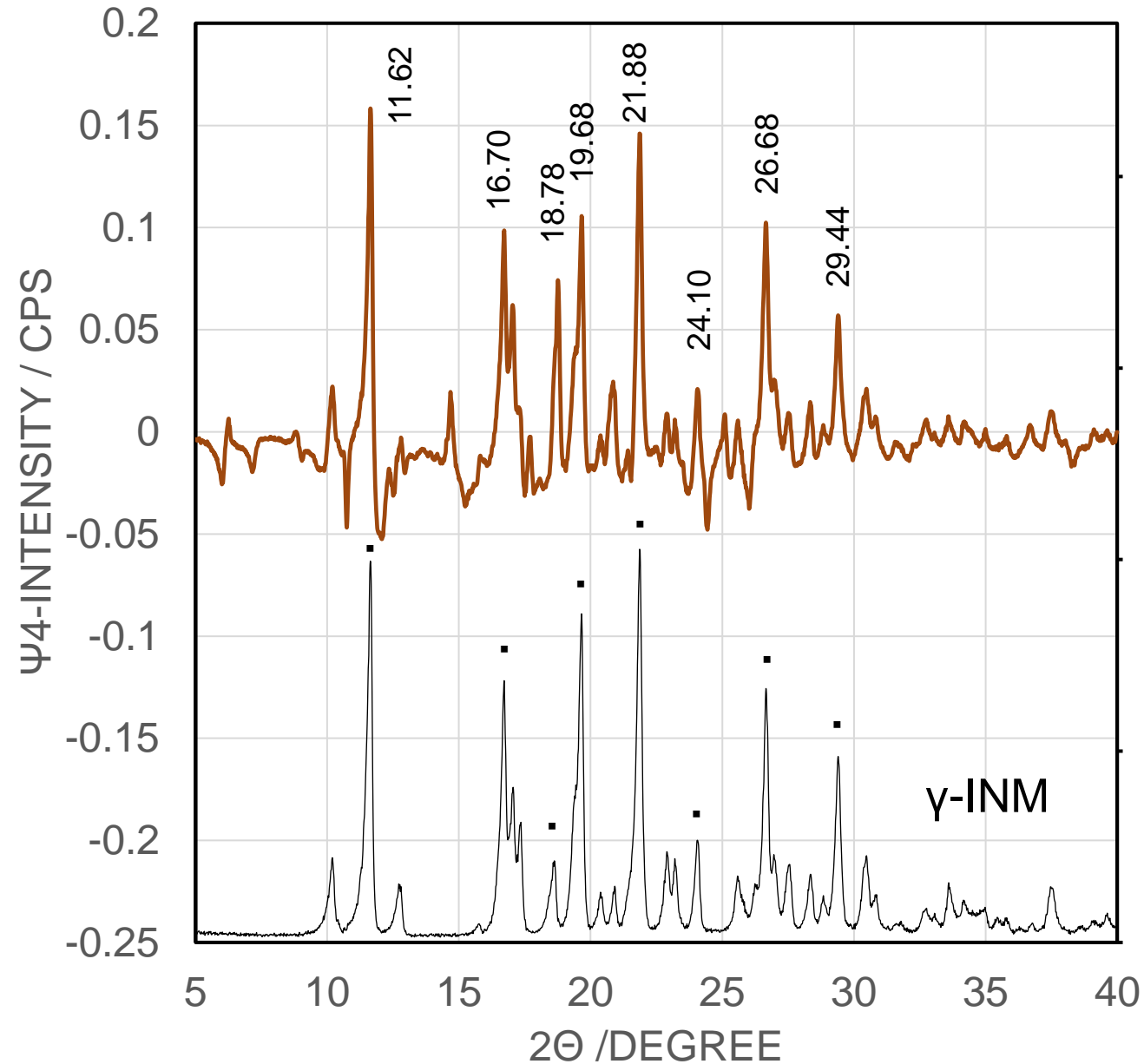
Figure S5(F) The 4-th singular vector (burgundy) compared with the diffractogram of INM γ-form (black)
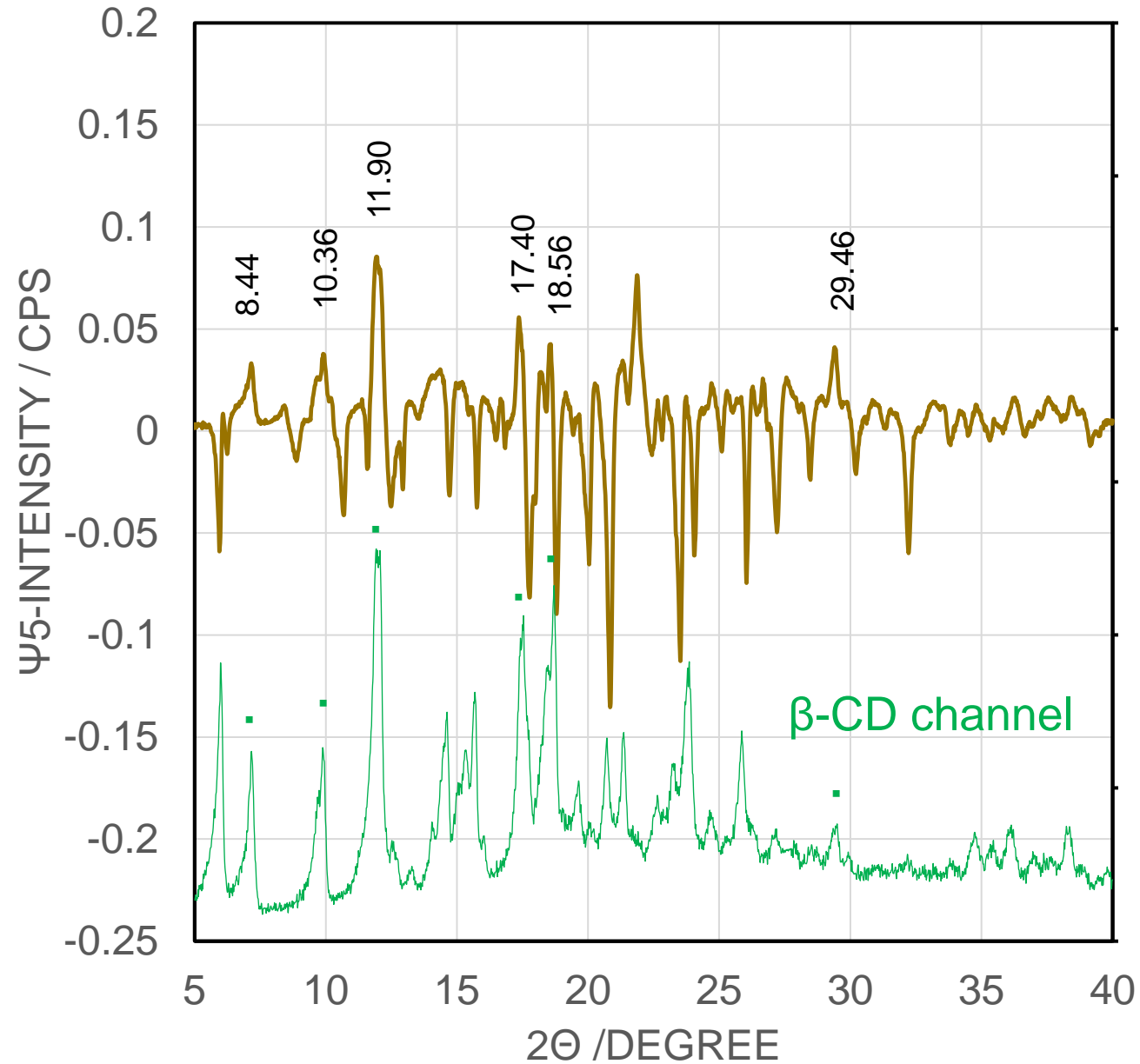
Figure S5(G) The 5-th singular vector (amber) compared with the pattern of β-CD channel-form (green) 24
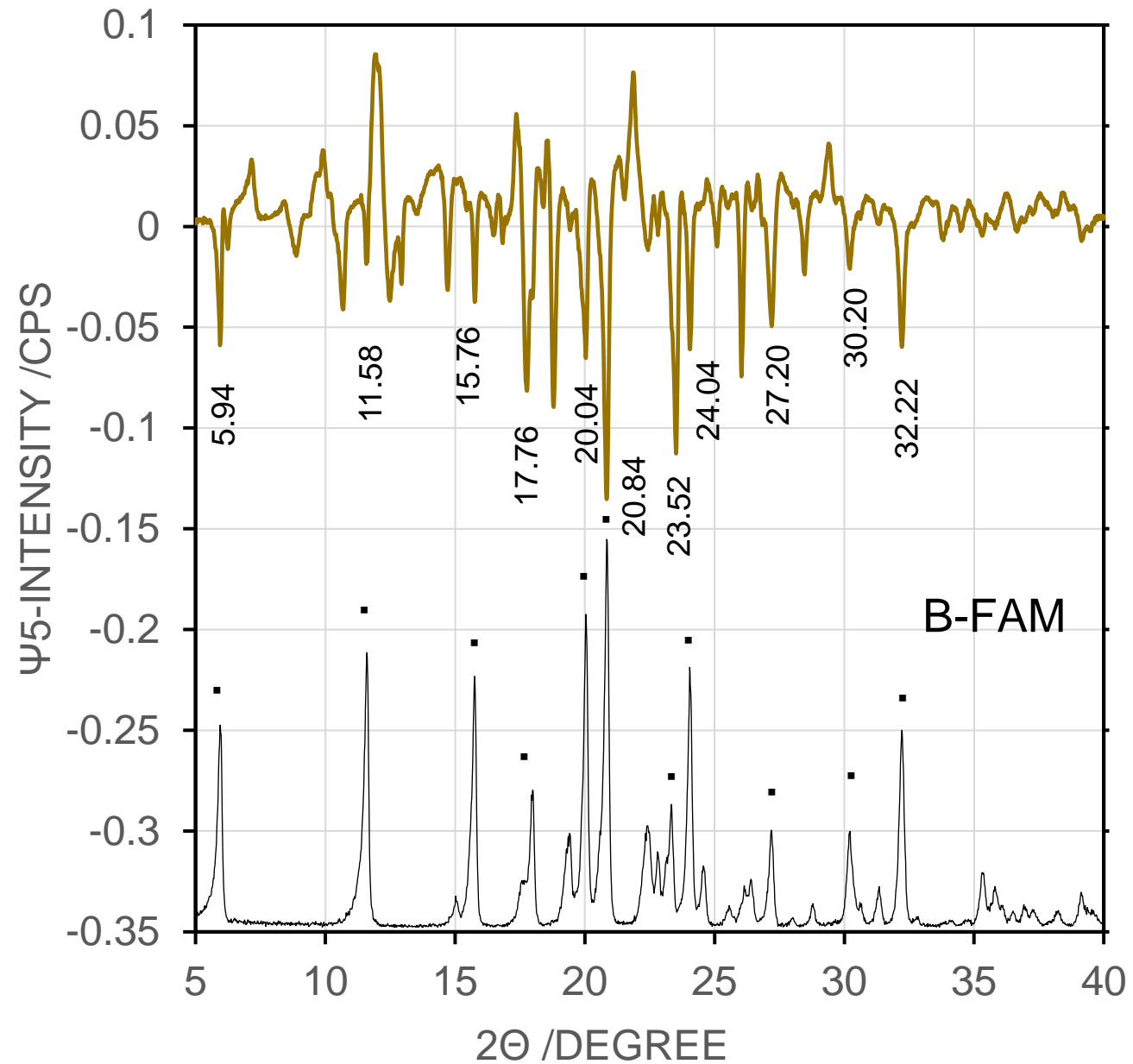
Figure S5(H) The 5-th singular vector (amber) compared with the diffractogram of INM γ-form (black)   25
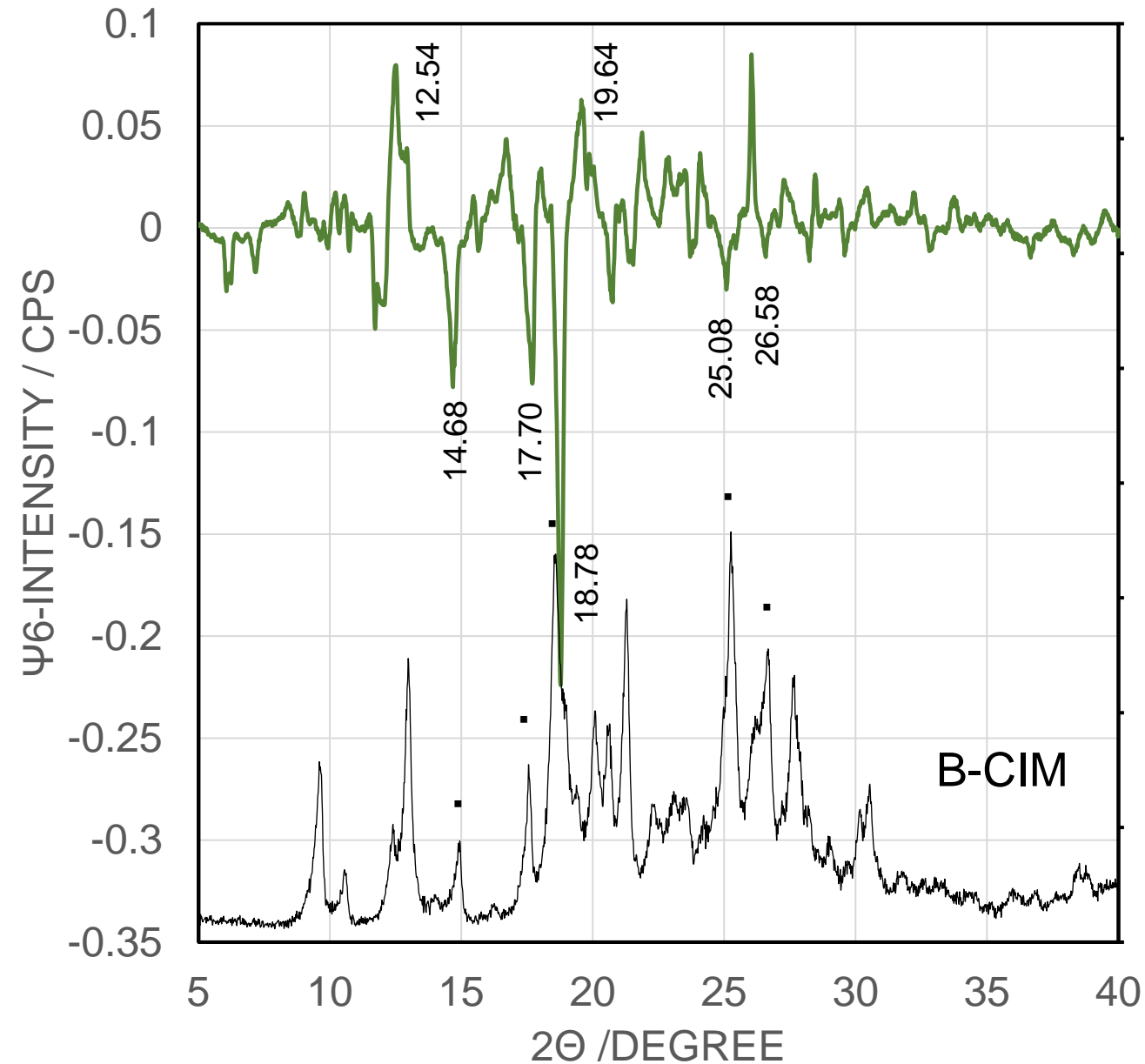
Figure S5(I) The 6-th singular vector (dark green) compared with the diffractogram of CIM B-form (black)
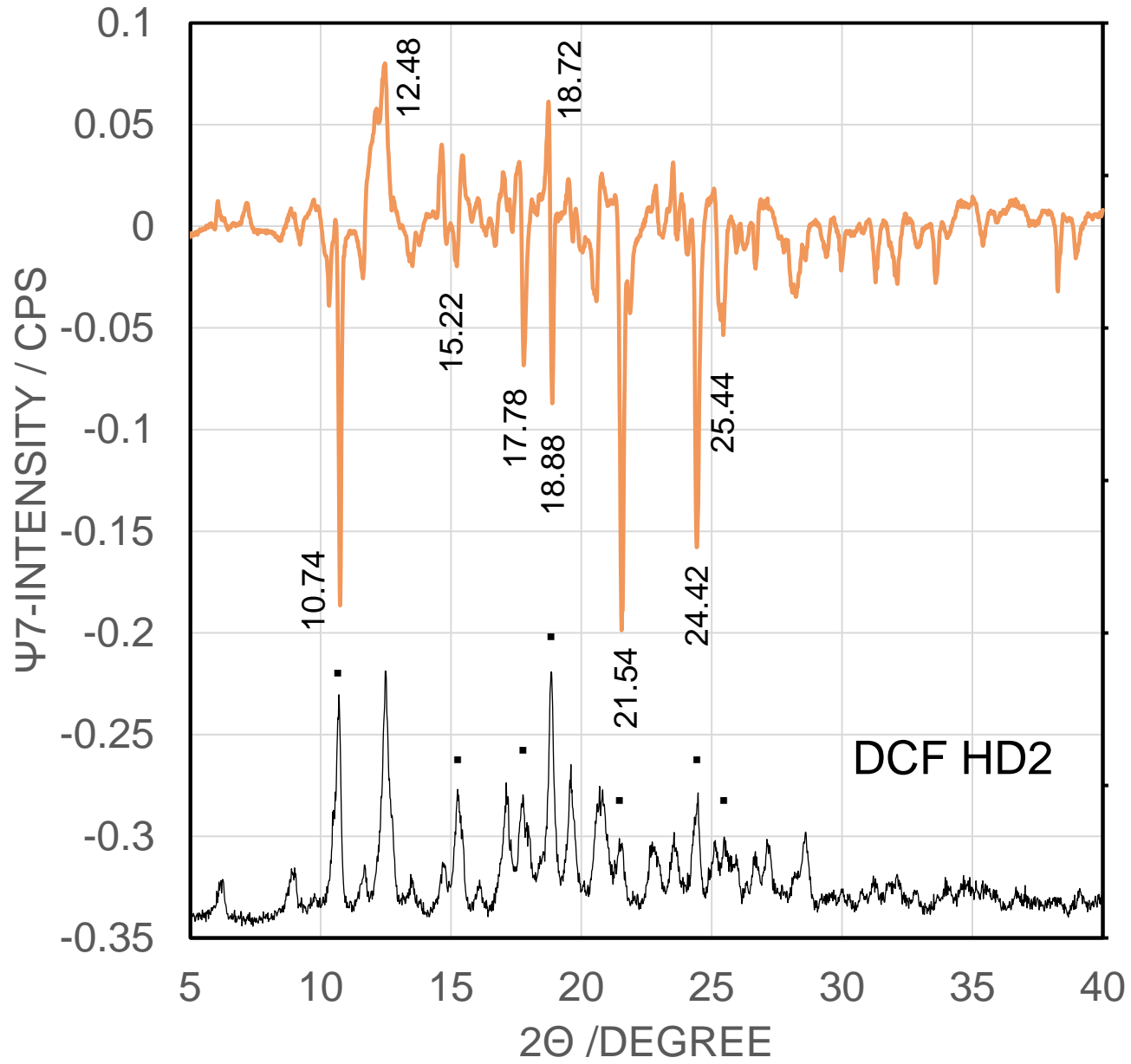
Figure S5(J) The 7-th singular vector (coral) compared with the diffractogram of DCF HD2-form (black)27
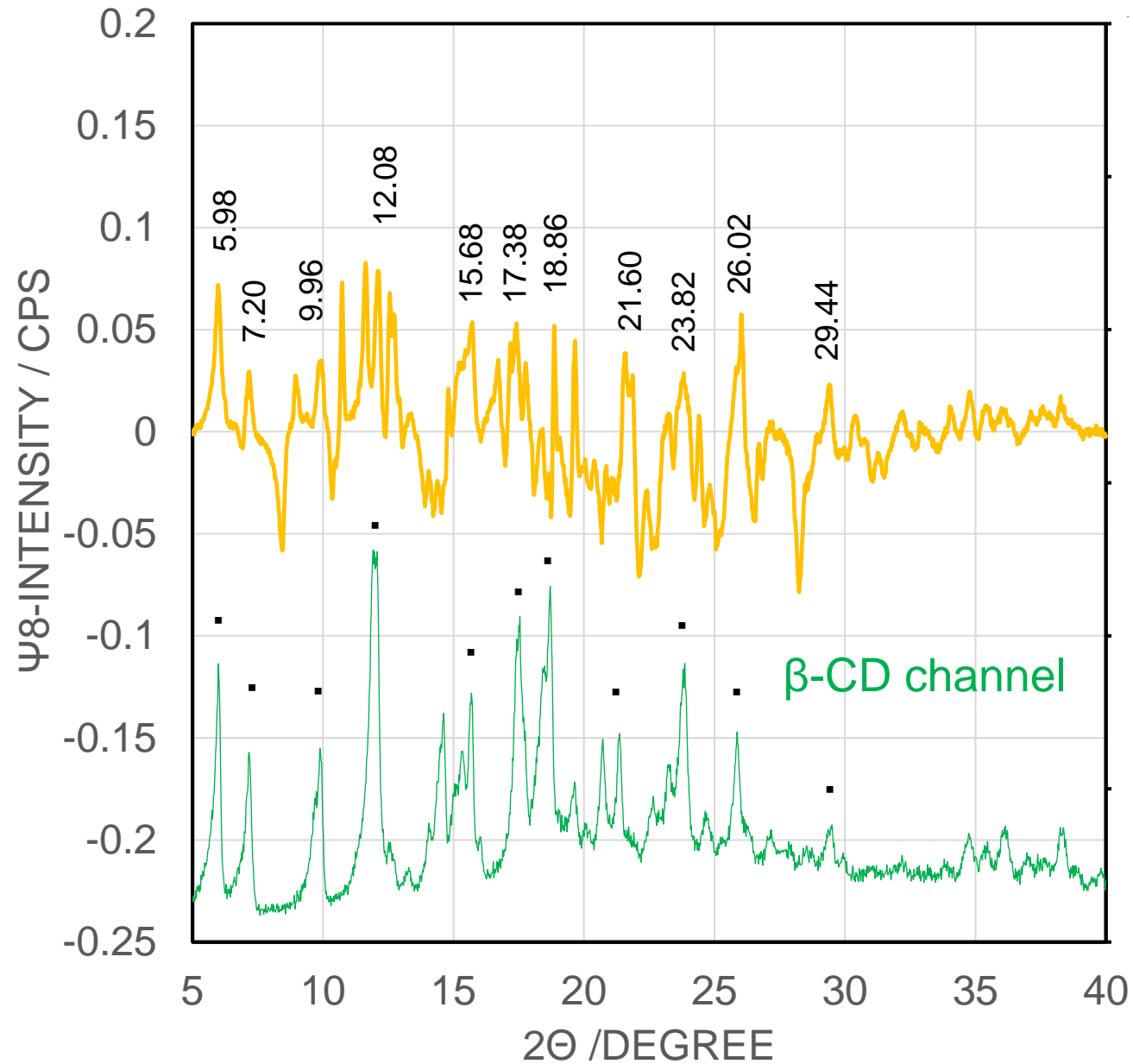
Figure S5(K) The 8-th singular vector (mustard) compared with the patern of β-CD channel-form (green)
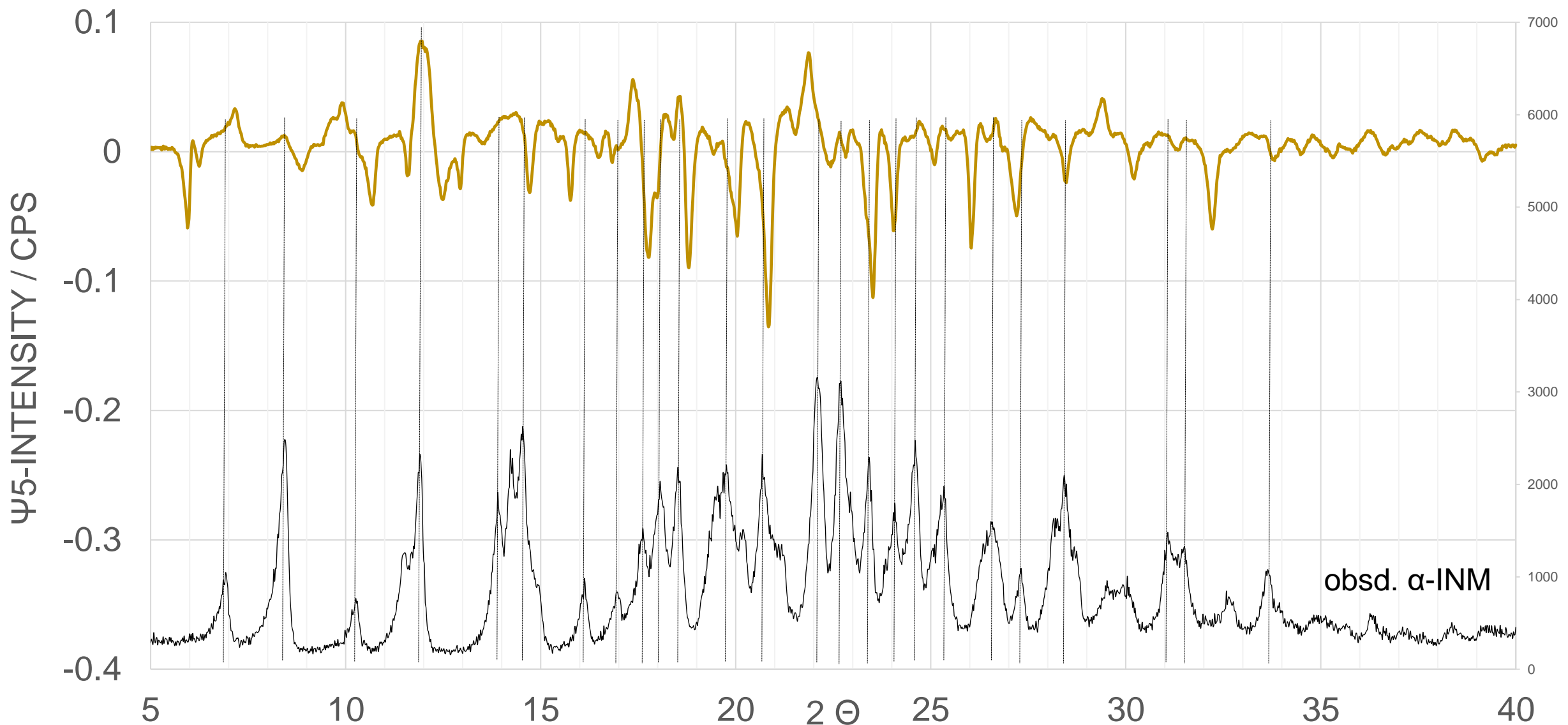
Figure S6. The 5-th basis function compared to the observed diffractogram of the INM α-form.
In the ψ5 (and other basis functions), neither peaks nor shoulders were almost found corresponding to those in the diffractogram of INM α-form.
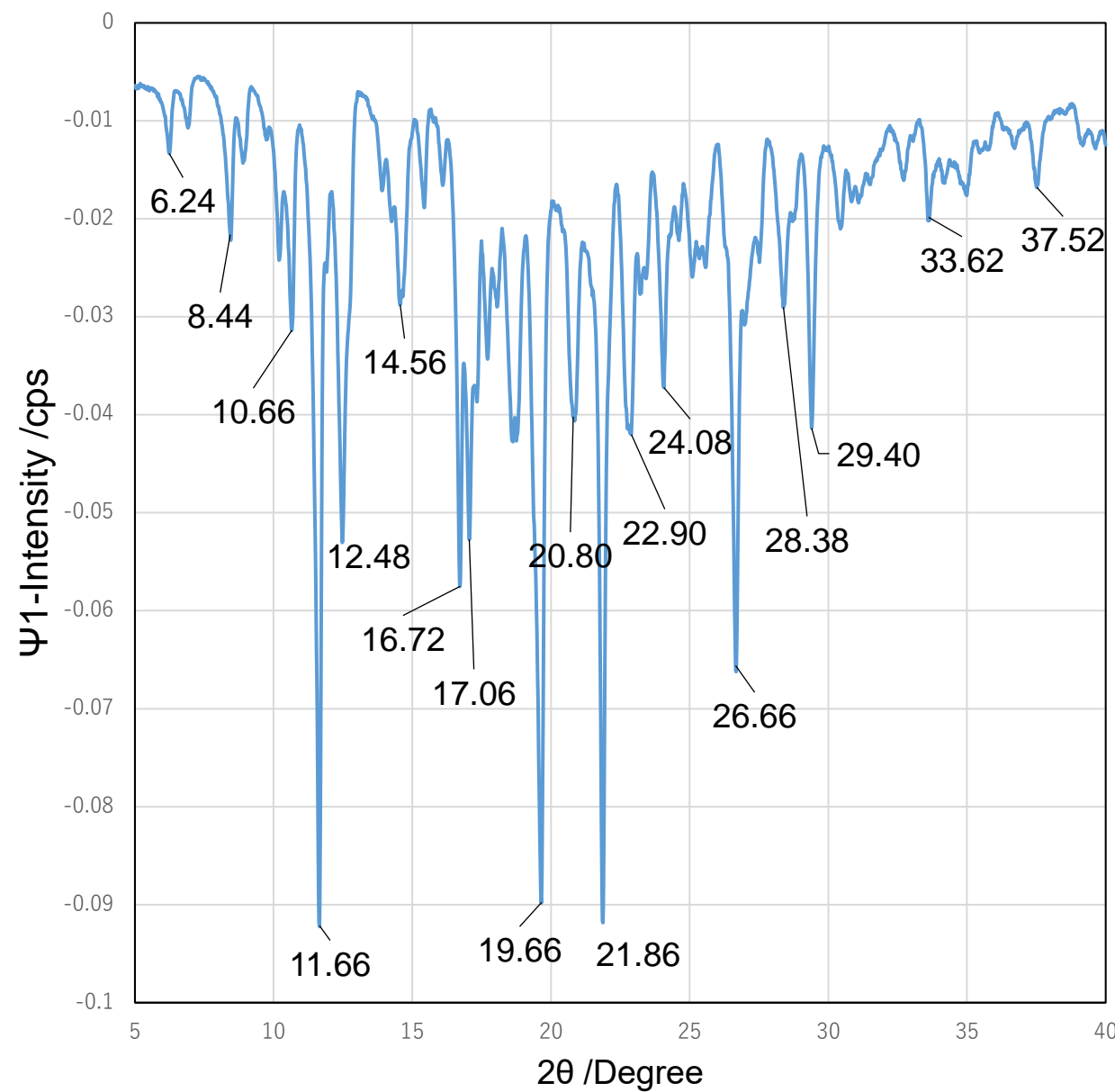
Figure S7(A) The 1-st singular vector (blue) in the SCD for the diffractograms of the INM/β-CD mixtures and the mixtures of the neat INM (γ-form) and its recrystallized α-form crystal at various molar ratios.
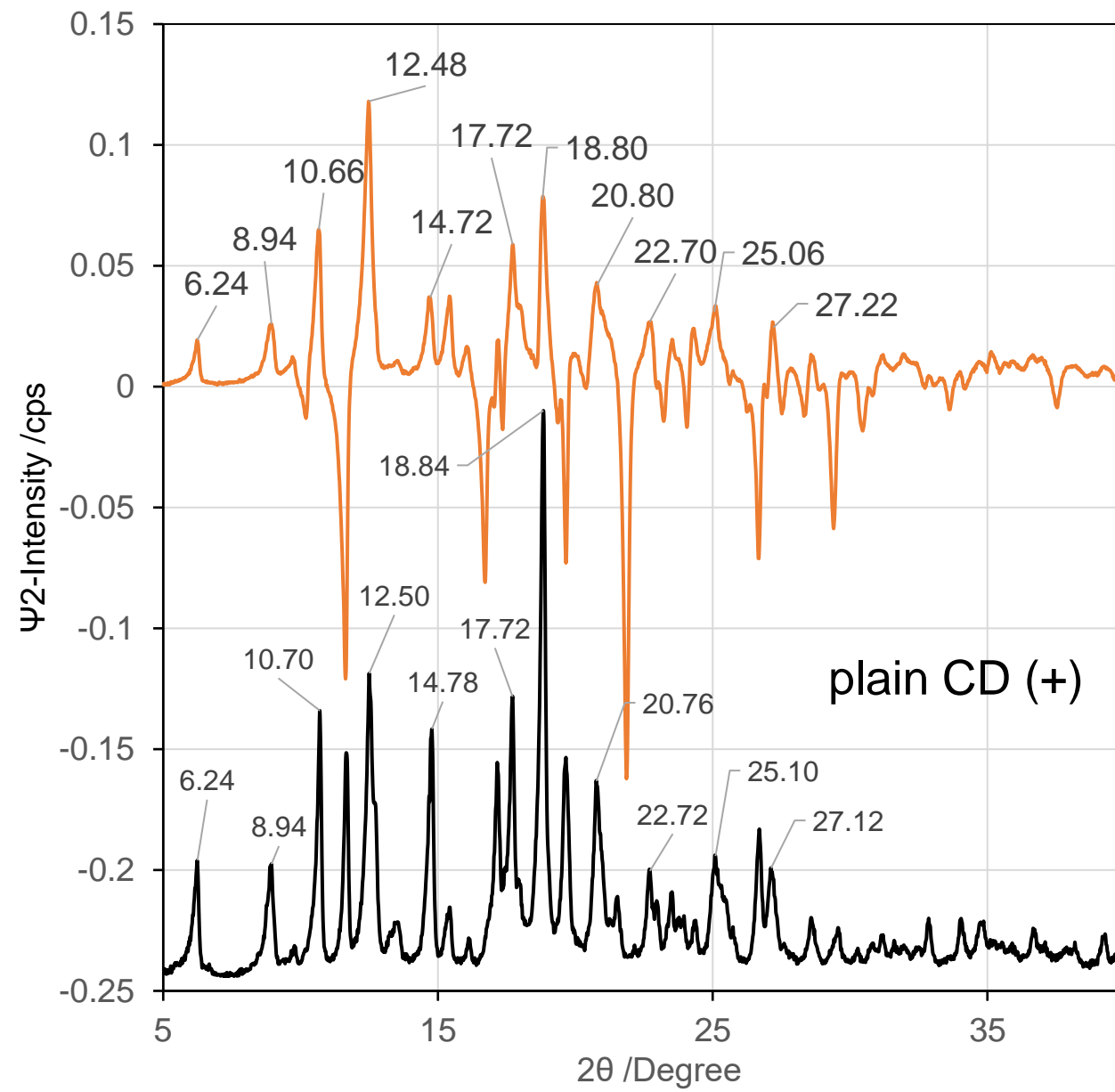
Figure S7(B) The 2-nd singular vector (orange) compared with the pattern of the plain β-CD (cage-form).
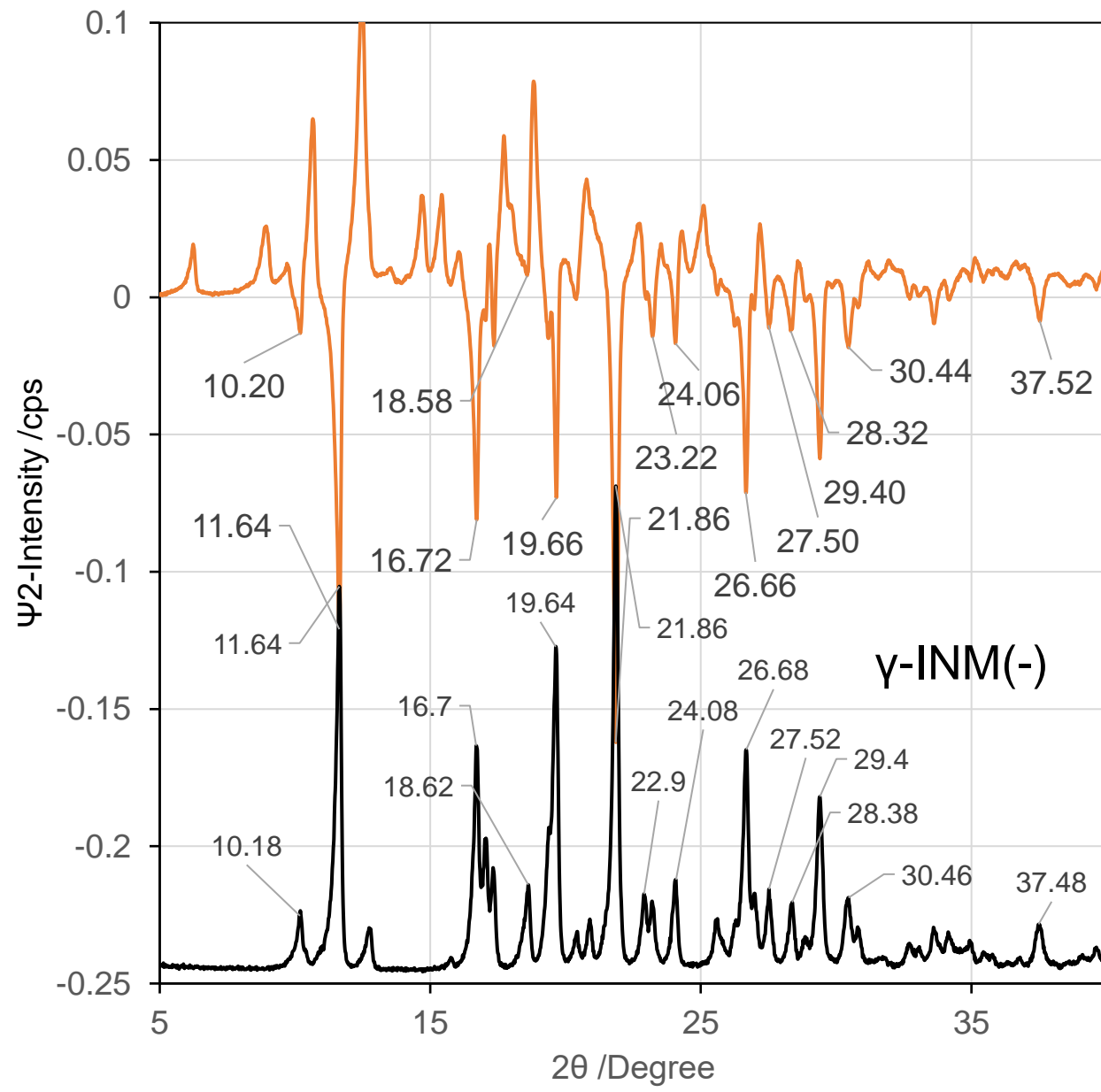
Figure S7(C) The 2-nd singular vector (orange) compared with the pattern of the neat INM (γ-form).
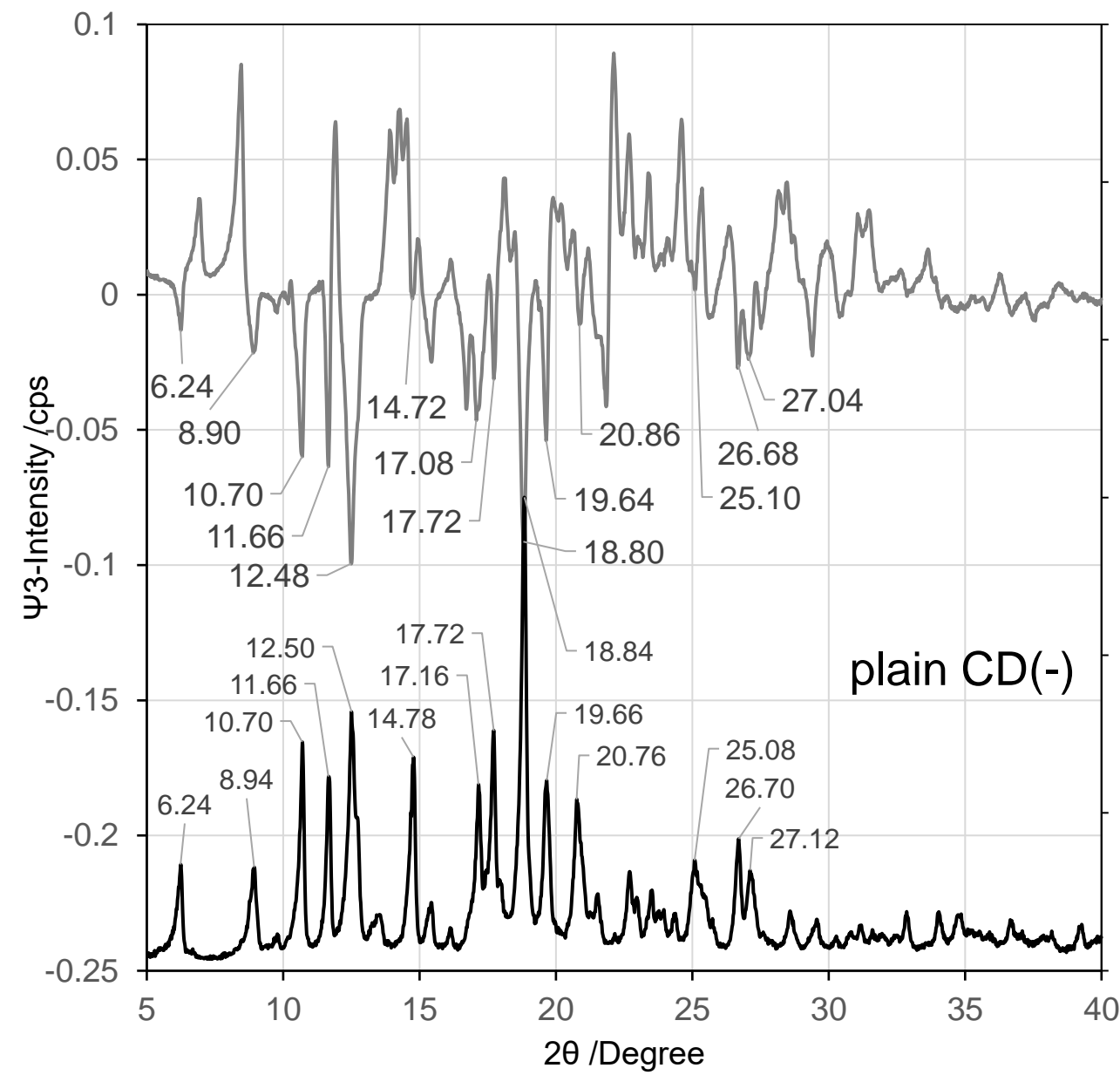
Figure S7(D) The 3-rd singular vector (gray) compared with the pattern of the plain β-CD (cage-form).
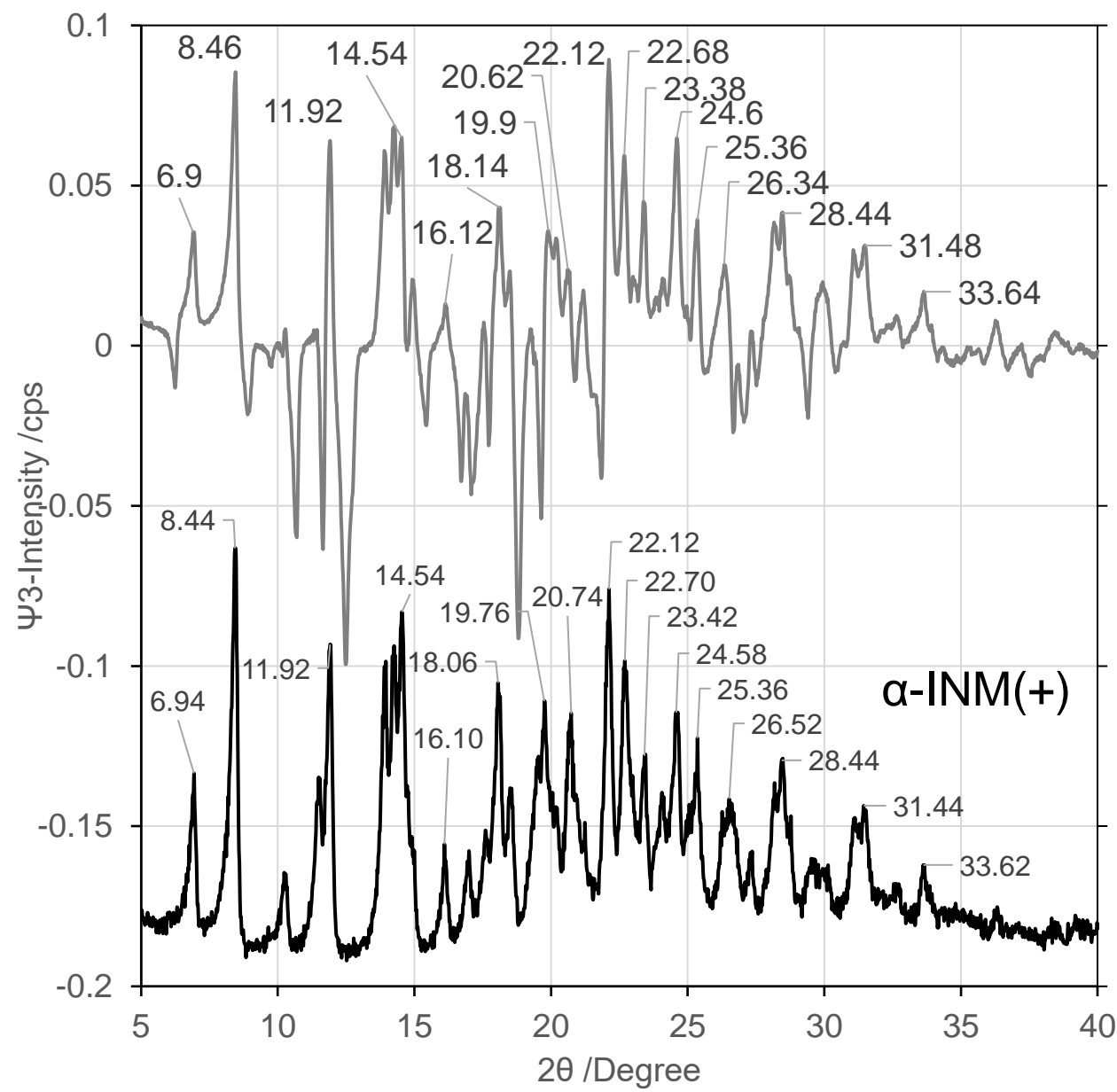
Figure S7(E) The 3-rd singular vector (gray) compared with the pattern of the recrystallized α-INM.
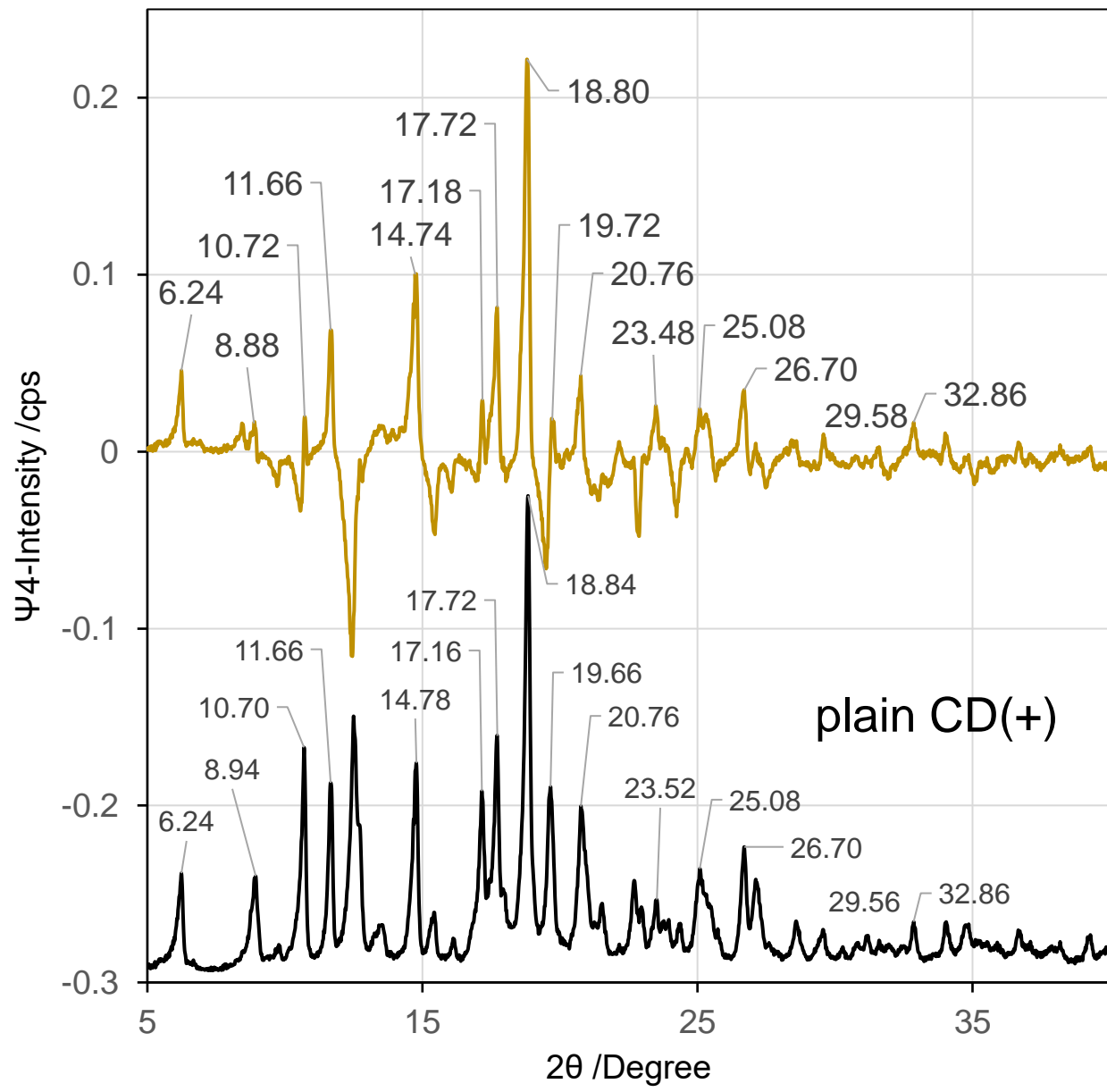
Figure S7(F) The 4-th singular vector (gray) compared with the pattern of the recrystallized α-INM.
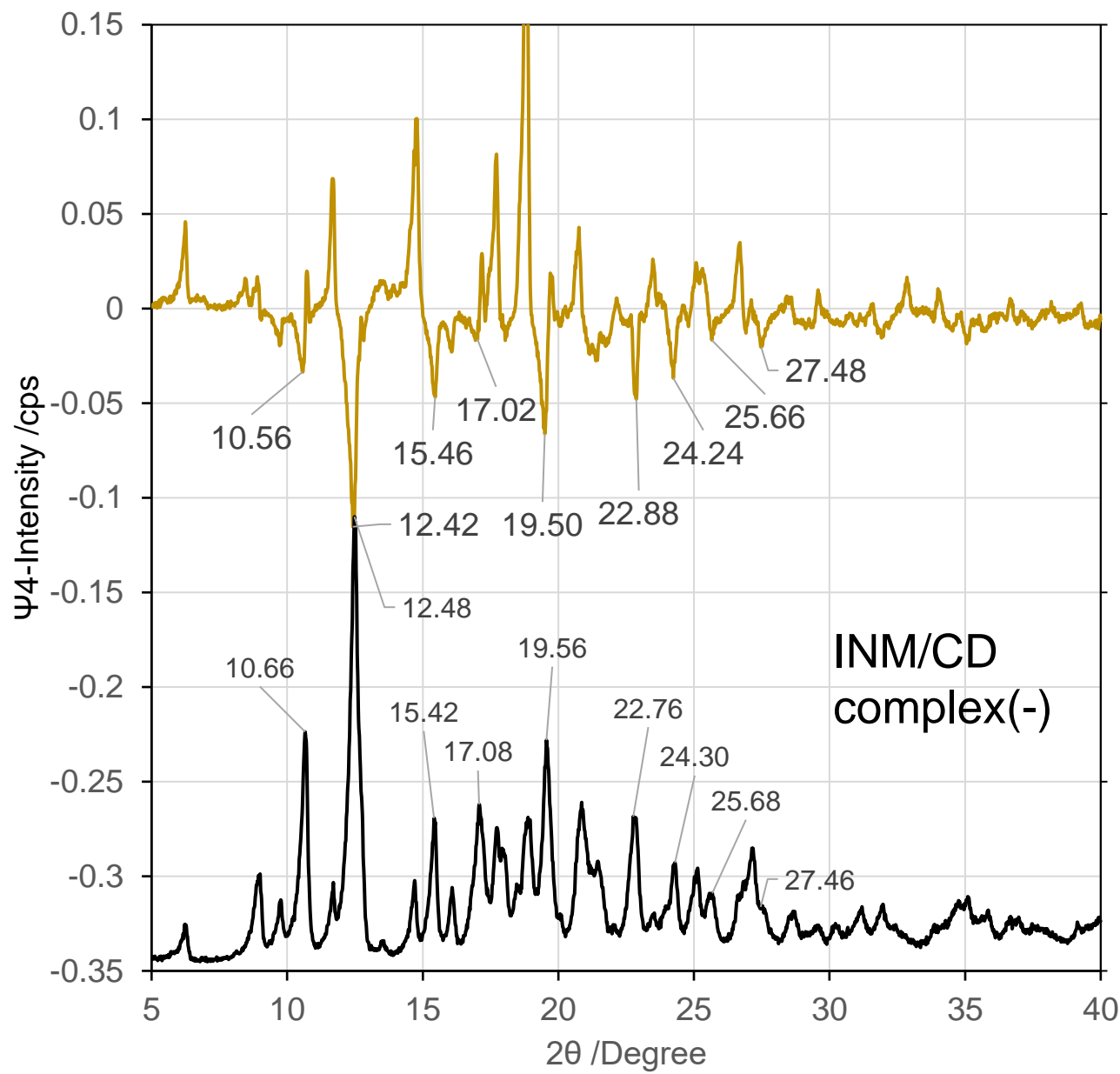
Figure S7(G) The 4-th singular vector (brown) compared with the pattern of the INM/CD complex/
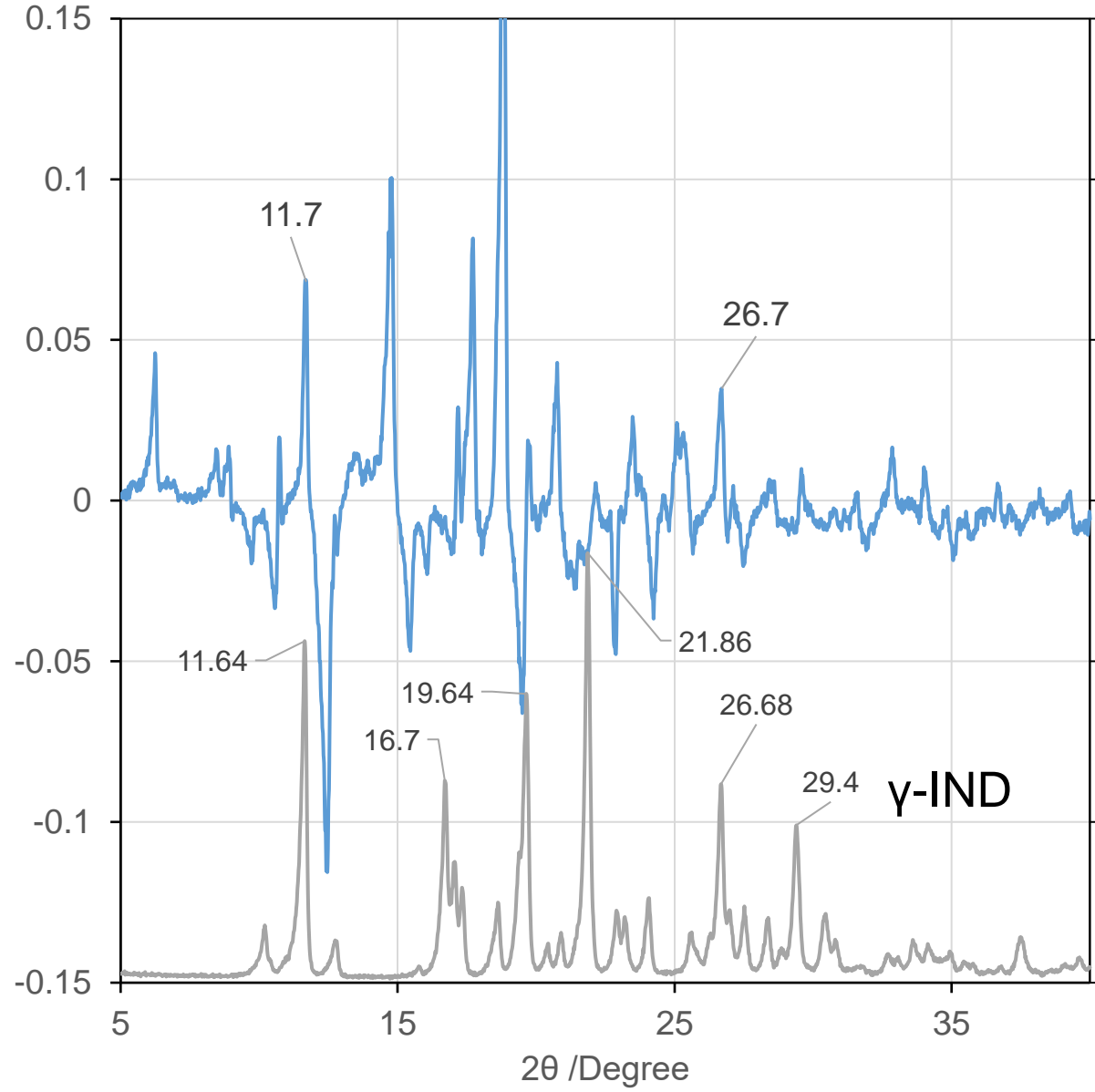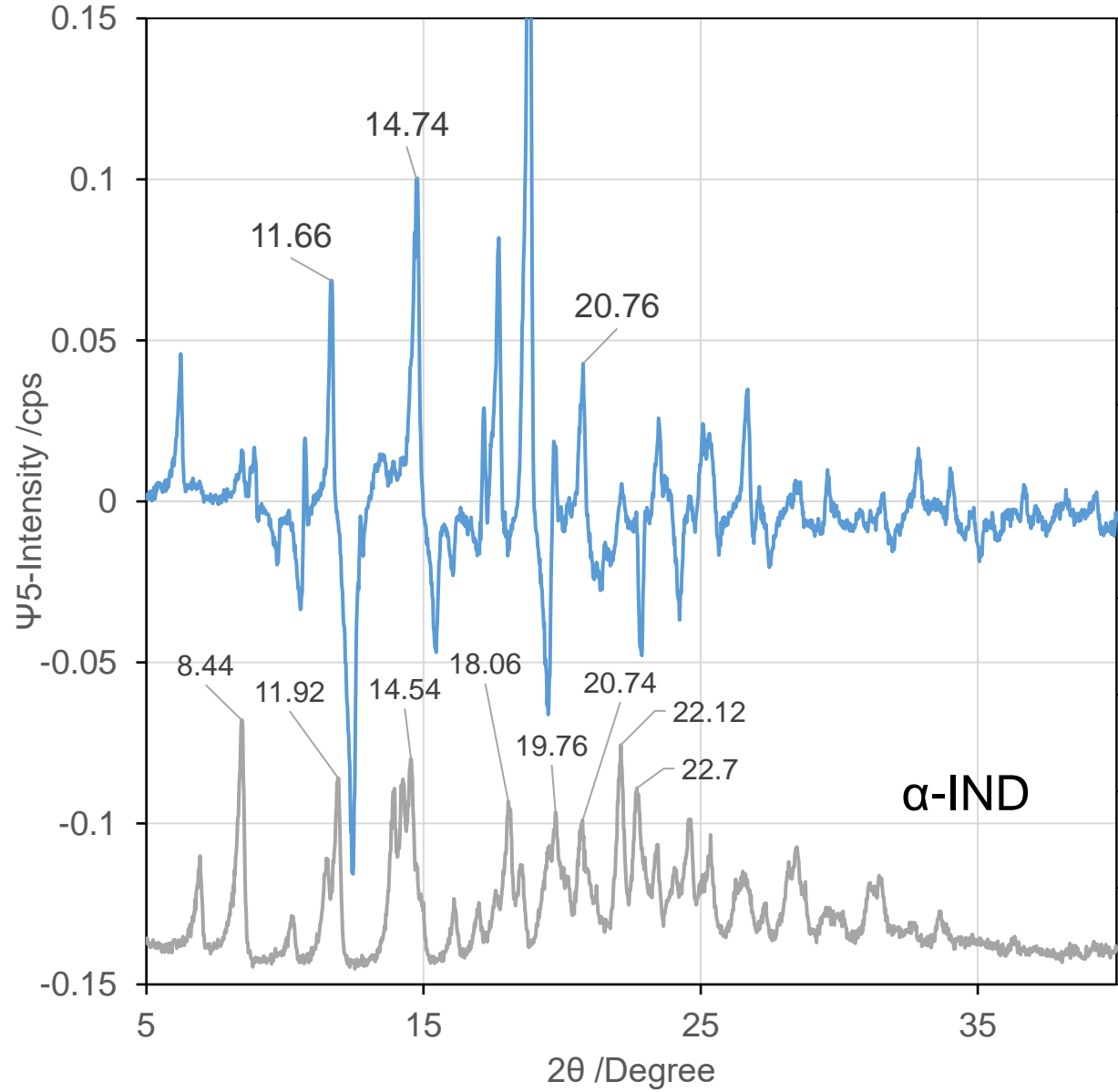
Figure S7(H) The 5-th singular vector (blue) compared with the patterns of the α- and γ-INM crystals.
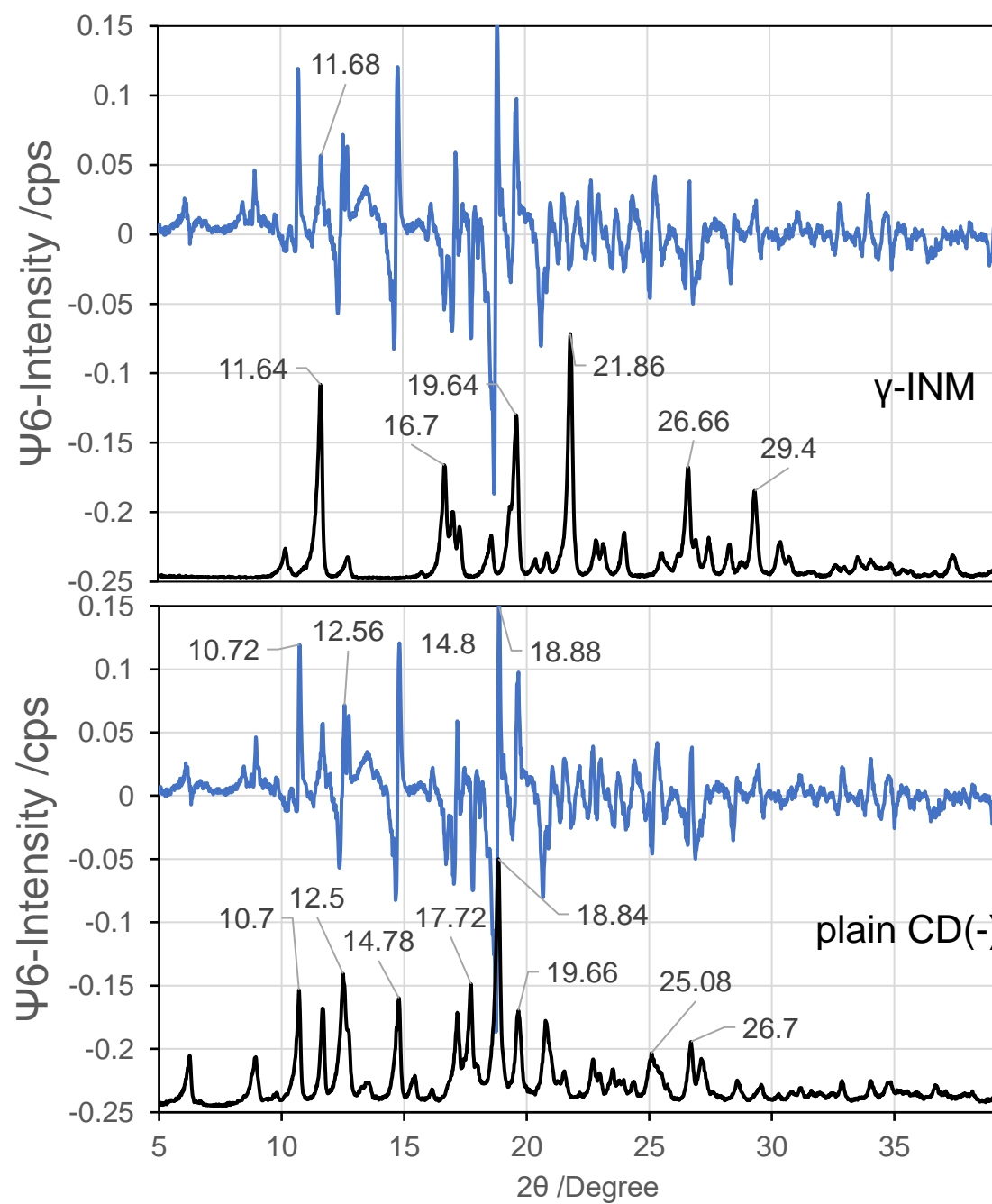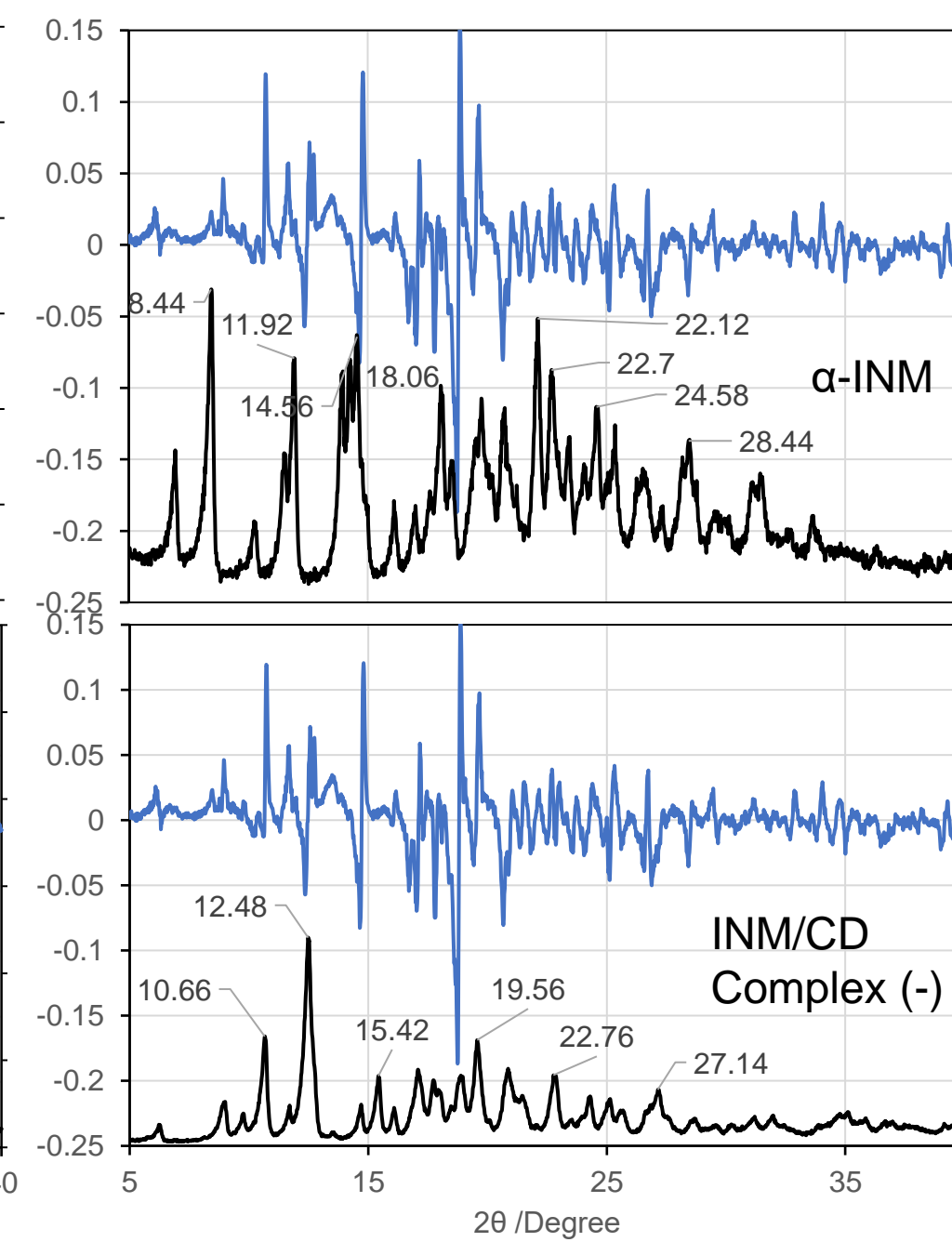
Figure S7(I) The 6-th singular vector (indigo) compared with the patterns of the INMs and CDs.
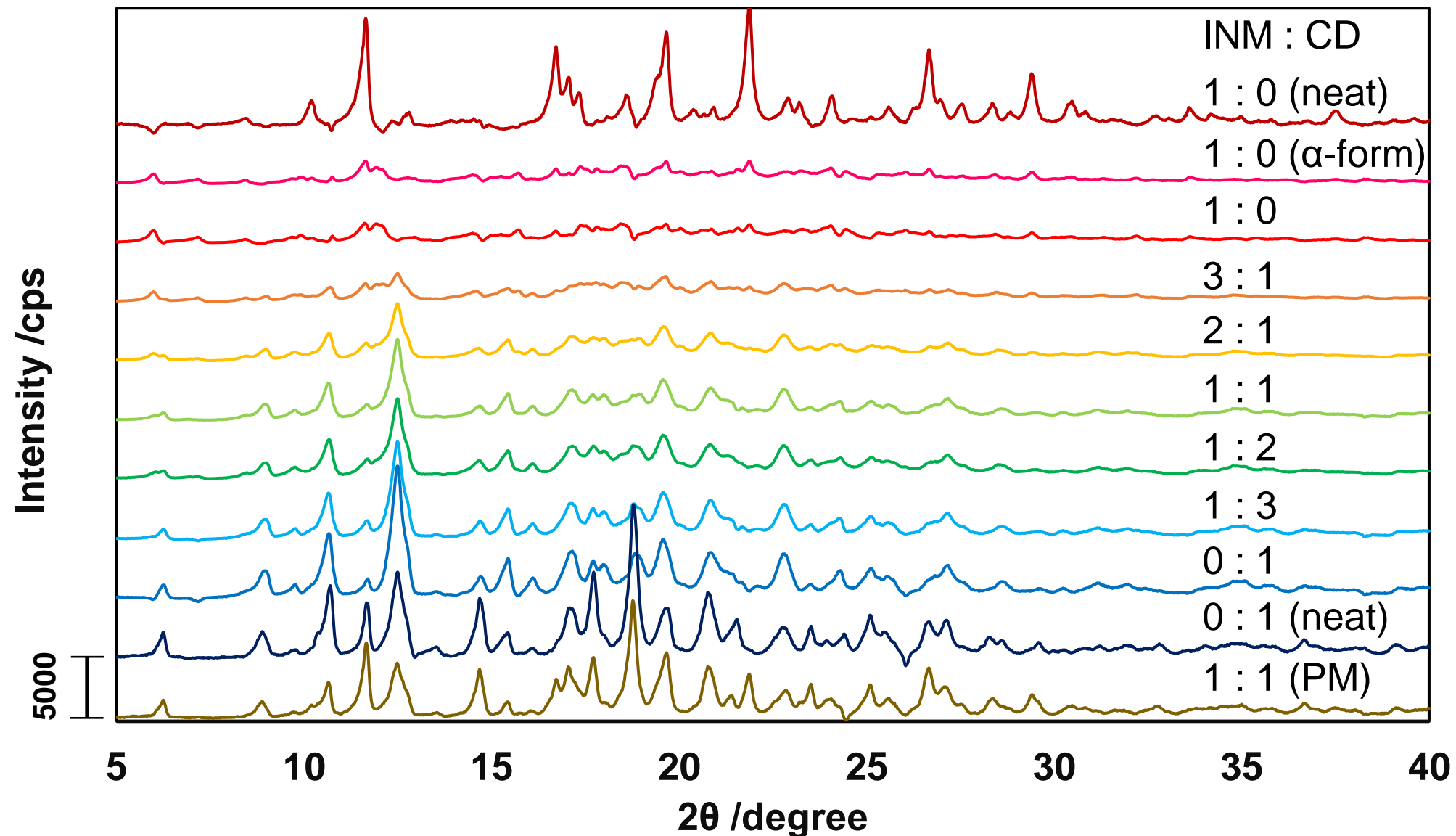
Figure S8 (A) Diffractograms of INM and their mixtures reproduced with 1st-7th components obtained by SVD on 1751 × 35 matrix. Those of neat INM (burgundy), α-INM (magenta), the SM-prepared INM/β-CD mixtures at various molar ratios, neat β-CD (indigo), and PM-treated INM/β-CD (brown).
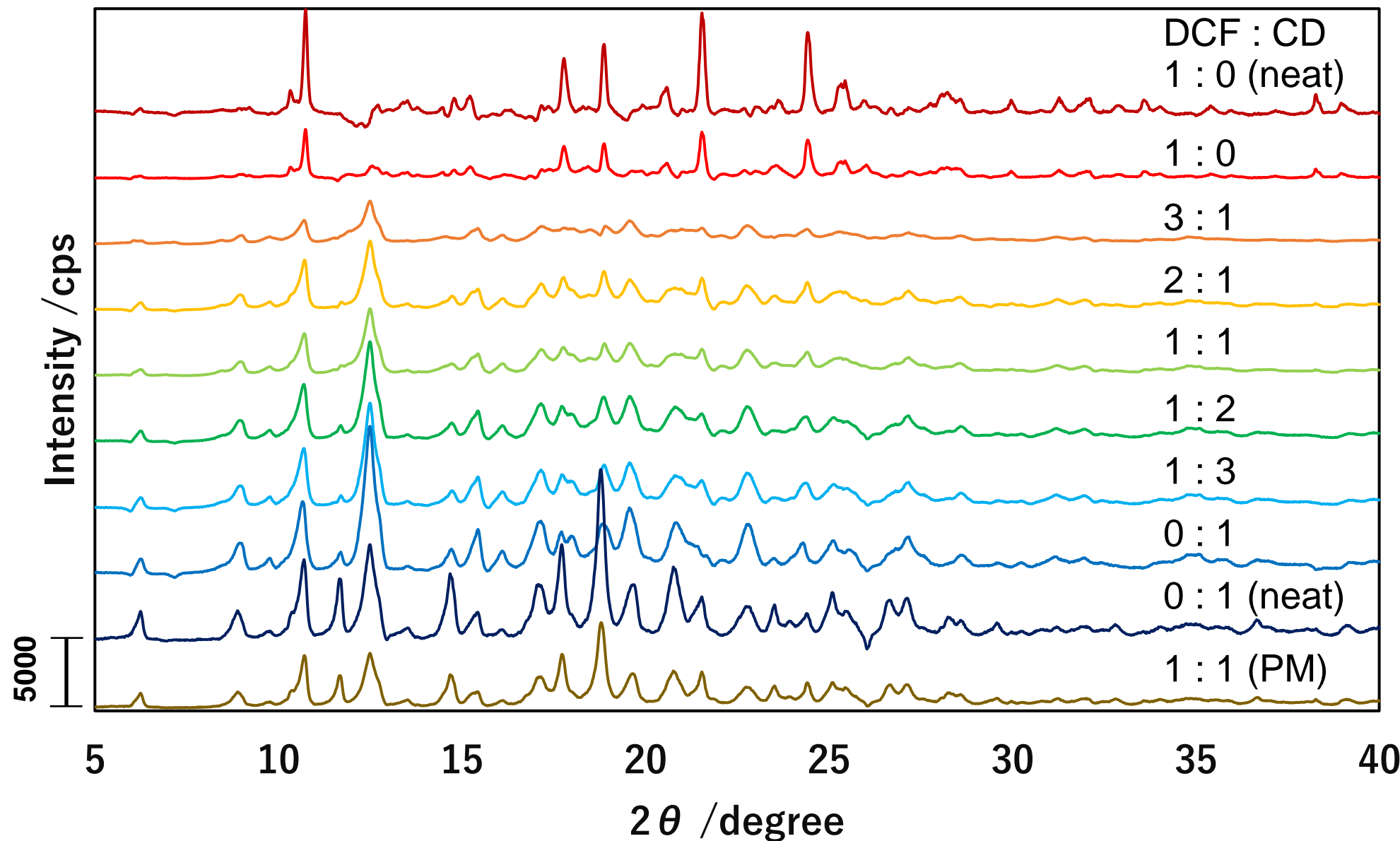
Figure S8 (B) Diffractograms of DCF and their mixtures reproduced with 1st-7th components obtained by SVD on 1751 × 35 matrix. Those of neat DCF (burgundy), the SM-prepared DCF/β-CD mixtures at various molar ratios, neat β-CD (indigo), and PM-treated DCF/β-CD (brown).
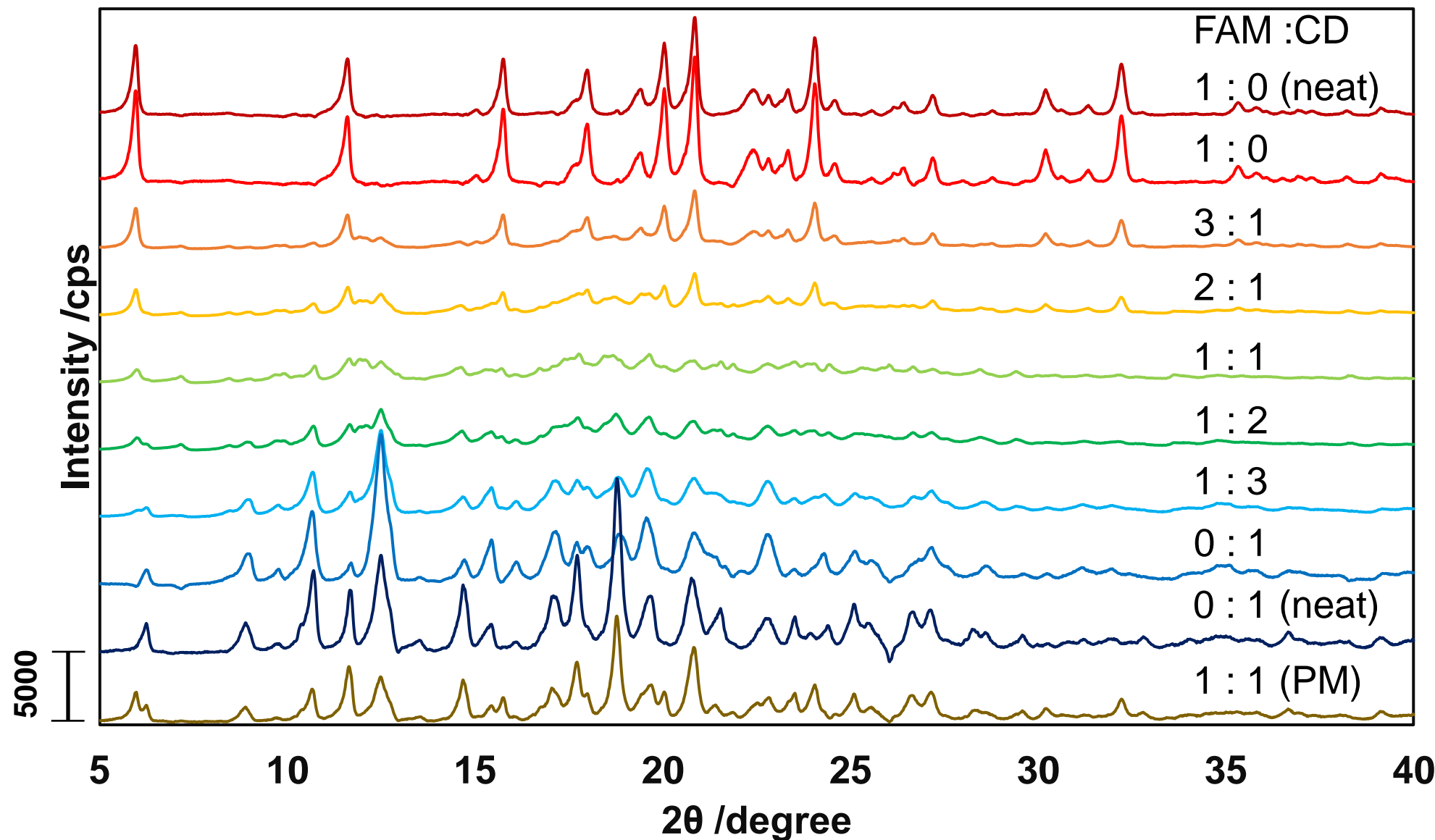
Figure S8 (C) Diffractograms of FAM and their mixtures reproduced with 1st-7th components obtained by SVD on 1751 × 35 matrix. Those of neat FAM (burgundy), the SM-prepared FAM/β-CD mixtures at various molar ratios, neat β-CD (indigo), and PM-treated FAM/β-CD (brown).
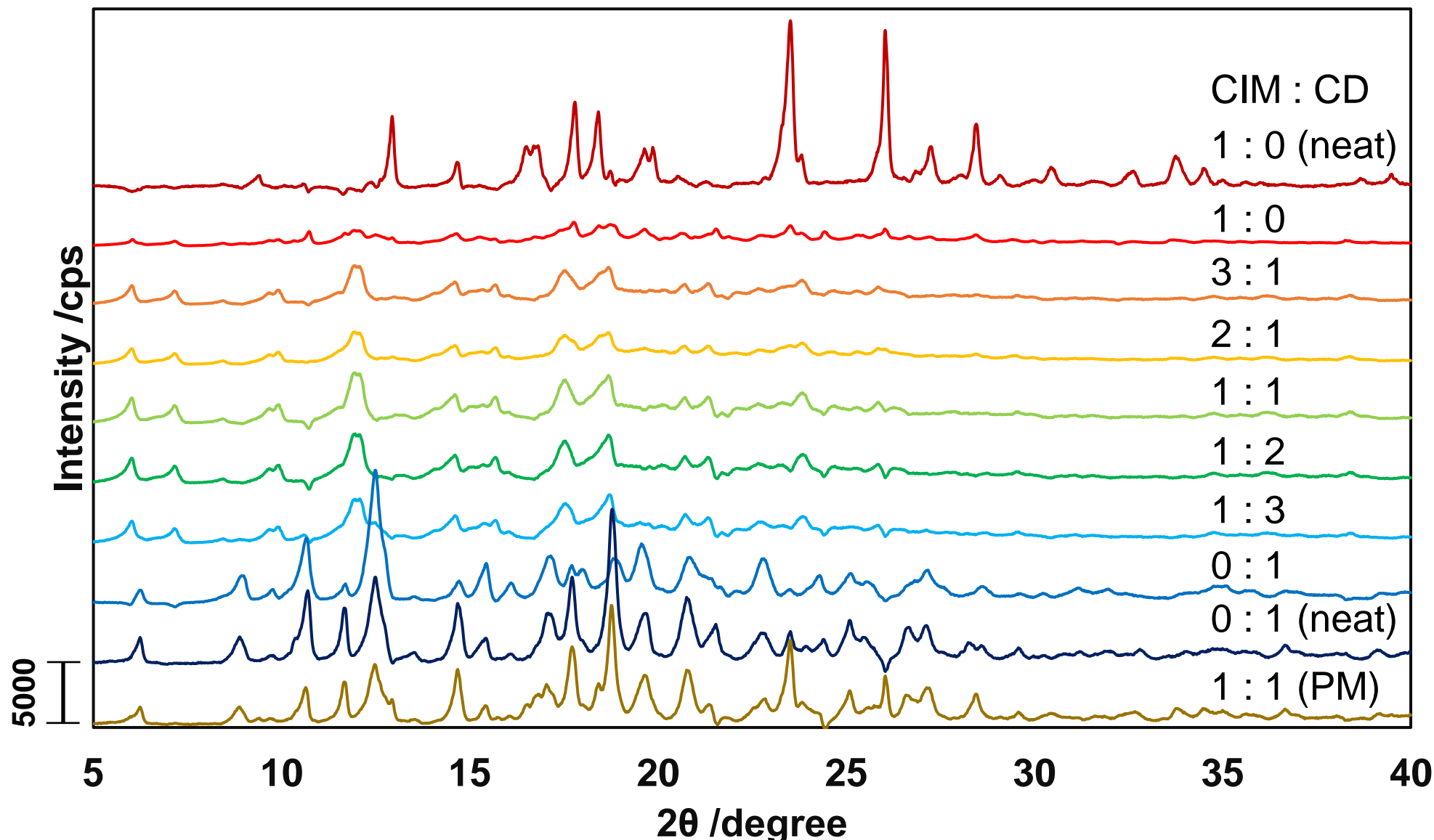
Figure S8 (D) Diffractograms of CIM and their mixtures reproduced with 1st-7th components obtained by SVD on 1751 × 35 matrix. Those of neat CIM (burgundy), the SM-prepared CIM/β-CD mixtures at various molar ratios, neat β-CD (indigo), and PM-treated CIM/β-CD (brown).